



KNUST

KWAME NKRUMAH UNIVERSITY OF SCIENCE AND TECHNOLOGY

COLLEGE OF ENGINEERING SCIENCES

DEPARTMENT OF MECHANICAL ENGINEERING

**THE EFFECT OF SETTLING HARMATTAN DUST ON
PHOTOVOLTAIC MODULES IN WALEWALE,
NORTHERN GHANA**

BY

OWUSU - BROWN BERNARD

(BSc Agricultural Engineering)

A THESIS SUBMITTED TO THE SCHOOL OF GRADUATE STUDIES, KWAME
NKRUMAH UNIVERSITY OF SCIENCE AND TECHNOLOGY, KUMASI, GHANA, IN
PARTIAL FULFILLMENT OF THE REQUIREMENT FOR THE AWARD OF
THE DEGREE OF MASTER OF SCIENCE IN MECHANICAL ENGINEERING

May, 2016

DECLARATION

I declare that this is a true result and reflection of my research work carried out in partial fulfillment of the requirement leading to the award of MSc. Mechanical Engineering Certificate. All citations and their sources have been duly acknowledged in the reference.

Any commission and omission with regards to this research is my responsibility herein signed below;

NAME

SIGNATORY

DATE

.....

I declare that I have supervised the student in undertaking the project reported herein and confirm that the student have my permission to present it for assessment

DR. ALBERT SUNNU

DATE

SIGNATORY

SUPERVISOR

.....

.....

PROF. F.K. FORSON

DATE

SIGNATORY

HEAD OF DEPARTMENT

.....

.....

DEDICATION

This project is dedicated to the almighty God who has been our strength and source of knowledge throughout our whole period of studies. To my lecturers, family and loved ones, God bless you all.



ACKNOWLEDGEMENT

As the author, I wish to acknowledge the support of all who have contributed directly or indirectly to this project. I thank the Almighty God who has divinely protected and guided me through this project work. I also acknowledge the immense contribution, guidance and support received from Dr. Albert Sunnu, who is my main Supervisor, Dr E. Ramde and Dr. Richard Opoku, for their assistance and advice. I also acknowledge Mr. Emmanuel Narh and Mr. Edwin who were the project leaders, for their guidance and expertise. To the Owusu-Brown's Family, Patricia Nyamekye-Nyantah and Rev. Tony Amoako-hene, God richly bless you all for your emotional and financial support.



ABSTRACT

Solar module performance is of high concern for dusty regions with less rainfall especially during the harmattan season in Ghana. The suspended harmattan dust scatters sunshine radiation before reaching the panel and upon settling on the panel surface, the dust particles block (partially) the solar cells from receiving the solar radiation, thus reducing the maximum capture efficiency of the photovoltaic module and its electrical energy output. This work seeks to address the effect of settling dust on sun radiation reaching the panel surface. The PV module for this research is a 50W mono-crystalline silicon. Experimental data of modules voltage, atmospheric dust concentration, irradiation and wind velocity were recorded for 4 months (November, 2014 – February, 2015) at project site, Walewale – northern Ghana and analyzed. Settling dust affected the module performance by reducing its power output by 28.7% and panel efficiency reduction by 5.6%.

A model for dust deposition and how it affects PV power output was also developed to better predict the power output and energy yields and to optimize the PV module, by ensuring cleaning schedules.

Keywords: PV module, harmattan dust, panel efficiency, settling dust, power output

TABLE OF CONTENTS

DECLARATION.....	II
DEDICATION.....	
III	
ACKNOWLEDGEMENT	
IV	
ABSTRACT	
V	
TABLE OF CONTENTS	VI
LIST OF FIGURES	IX
LIST OF TABLES	X
ACRONYMS AND ABBREVIATIONS	
XI	
CHAPTER ONE	
I	
1.0 INTRODUCTION.....	1
1.1 BACKGROUND	1
1.2 STUDY AREA	4
1.3 JUSTIFICATION OF RESEARCH	4
1.4 OBJECTIVES	4
1.5 STRUCTURE OF THESIS	5
CHAPTER TWO	6
2.0 LITERATURE REVIEW	6

2.1	SOLAR PHOTOVOLTAIC SYSTEMS	6
2.1.2	COMPONENTS OF PV SYSTEM THAT PROVIDE SOLAR POWER:	8
2.2	THEORETICAL MODELLING OF SOLAR CELL	8
2.2.1	POWER OUTPUT OF CELL	11
2.2.2	EFFICIENCY OF PV CELL	11
2.2.3	STANDARD TEST CONDITIONS (STC)	12
2.3	THEORETICAL CONSIDERATIONS OF DUST	12
2.4	DUST DEPOSITION	14
2.4.1	FACTORS AFFECTING DUST SETTLEMENT ON PV PANEL	15
2.4.2	MECHANISM OF DUST DEPOSITION	16
2.4.3	STOKE'S SETTLING	18
2.4.4	ADHESION OF DUST PARTICLE	20
2.5	EFFECT OF DUST ON PV CELL PERFORMANCE	23
2.6	EFFECT OF DUST ON THE I-V OUTPUTS OF A PANEL	25
CHAPTER THREE		26
3.0	METHODOLOGY	26
3.1	OBJECTIVE 1	26
3.1.1	METHODOLOGY	26
3.1.2	FIELD MEASUREMENTS	27
3.1.3	SENSOR'S CONFIGURATION	34
3.1.4	PHOTOVOLTAIC SYSTEM	34
3.2	OBJECTIVE 2 AND OBJECTIVE 3	37
3.2.1	METHODOLOGY	37

3.3	OBJECTIVE 5	38
3.4.1	METHODOLOGY	38
3.4.2	MATHEMATICAL MODULE	41
CHAPTER FOUR	43
4.0	RESULTS AND DISCUSSION	43
4.1	OBJECTIVE 1	43
4.1.1	RESULTS AND DISCUSSION	43
4.2	OBJECTIVE 2	47
4.2.1	RESULTS AND DISCUSSION	47
4.3	OBJECTIVE 3	48
4.3.1	RESULTS AND DISCUSSION	48
4.4	OBJECTIVE 4	51
4.4.1	RESULTS AND DISCUSSION	51
4.5	OBJECTIVE 5	52
4.5.1	RESULTS AND DISCUSSION	52
4.5.2	MODELLING THE EFFECT OF SAMPLED ATMOSPHERIC DUST PARTICLES AND WIND SPEED ON THE PANEL POWER OUTPUT	53
CHAPTER FIVE	57
5.0	CONCLUSION AND RECOMMENDATION	57
5.1	CONCLUSIONS	58
5.2	RECOMMENDATIONS	58
REFERENCES	59

APPENDIX A	63
APPENDIX B	64
APPENDIX C	65

LIST OF FIGURES

<i>Figure.1.1. How dust affects the output of a panel.....</i>	<i>3</i>
<i>Figure.2.1. Photovoltaic system.....</i>	<i>6</i>
<i>Figure.2.2. Circuit diagram of the PV model.....</i>	<i>8</i>
<i>Figure.2.3. Factors affecting dust settlement.....</i>	<i>16</i>
<i>Figure.2.4. Free body diagram of a spherical particle in a viscous fluid.....</i>	<i>19</i>
<i>Figure.2.5. Spherical particle rests on ideally flat surface.....</i>	<i>22</i>
<i>Figure.3.1. The Automatic Weather Station at Walewale.....</i>	<i>27</i>
<i>Figure 3.2. The dust monitor sensor.....</i>	<i>27</i>
<i>Figure 3.3. Forward Laser Light Scatter Nephelometer System.....</i>	<i>30</i>
<i>Figure.3.4. ES-642 Airflow System Diagram.....</i>	<i>33</i>
<i>Figure 3.5. The photovoltaic system.....</i>	<i>36</i>
<i>Figure.3.6. Interactions between dust and panel surface and itself.....</i>	<i>40</i>
<i>Figure 4.1. The effect of dust on panel efficiency.....</i>	<i>47</i>
<i>Figure 4.2. Impact of settling dust on current output.....</i>	<i>48</i>
<i>Figure 4.3. Factors that influences panel voltage output</i>	<i>49</i>
<i>Figure.4.4. Experimental IV-Curve representation.....</i>	<i>50</i>
<i>Figure.4.5. Relationship between Irradiation and Panel Power Output.....</i>	<i>51</i>
<i>Figure 4.6. Effect of settling dust and wind velocity on panel power output.....</i>	<i>52</i>
<i>Figure 4.7. Comparing the power output of the panel</i>	<i>55</i>
<i>Figure 4.8. Residual plots of the linear modules.....</i>	<i>56</i>

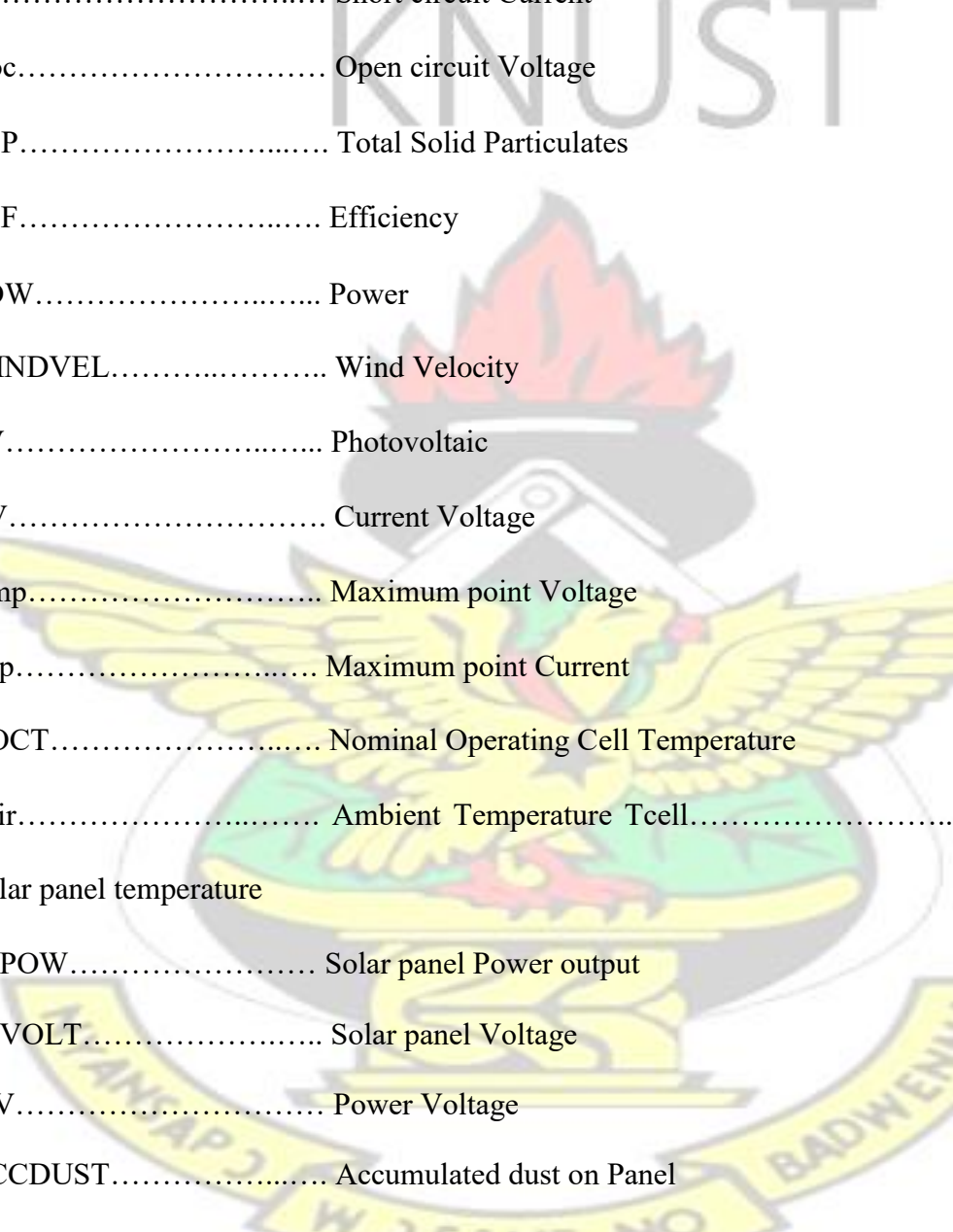
LIST OF TABLES

<i>Table 2.1 Configuration of the installed sensors at the weather station.....</i>	<i>34</i>
---	-----------

<i>Table 3.1 The Physical characteristics of the panel.....</i>	<i>35</i>
<i>Table 3.2 The Electrical Characteristics of the panel.....</i>	<i>35</i>
<i>Table.4.1. Tabulated experimental data.....</i>	<i>43</i>
<i>Table.4.2. Values of efficiency measured and calculated.....</i>	<i>54</i>



ACRONYMS AND ABBREVIATIONS



SP.....	Solar Panel
Isc.....	Short circuit Current
Voc.....	Open circuit Voltage
TSP.....	Total Solid Particulates
EFF.....	Efficiency
POW.....	Power
WINDVEL.....	Wind Velocity
PV.....	Photovoltaic
I-V.....	Current Voltage
Vmp.....	Maximum point Voltage
Imp.....	Maximum point Current
NOCT.....	Nominal Operating Cell Temperature
Tair.....	Ambient Temperature Tcell.....
Solar panel temperature	
SPPOW.....	Solar panel Power output
SPVOLT.....	Solar panel Voltage
P-V.....	Power Voltage
ACCDUST.....	Accumulated dust on Panel
V.....	Voltage
DC.....	Direct current
GHI.....	Global Horizontal Irradiation

A.W.S..... Automatic Weather Station

KNUST



CHAPTER ONE

1.0 INTRODUCTION

In this chapter, the background, problem statement, objectives and significance of the research and structure of the thesis were discussed.

1.1 BACKGROUND

The renewable energy sources which are also called non-conventional energy resources are the sources which are continuously renewed by natural processes. They include solar energy, bio-energy, wind energy, ocean energy, tidal energy, hydropower, etc. A renewable energy system converts the energy found in sunlight, falling-water, wind, sea-waves, geothermal heat, or biomass into a usable form, in the form of heat energy or electrical energy. The majority of the renewable energy is derived directly or indirectly from the sun and wind.

However, in the modern world, majority of the world's energy sources are from the conventional sources (non-renewable) - fossil fuels such as coal, natural gases and petroleum. Renewable energy resources exist over wide geographical areas, in contrast to other energy sources, which are concentrated in a limited number of countries. Rapid development of renewable energy, energy efficiency and technological diversification of energy sources, would result in significant energy security and economic benefit for the country (IEA, 2012).

Solar energy as a form of renewable energy has been harnessed by humans since ancient times using a variety of technologies. To harvest solar energy, the most common

way is to use photovoltaic panels which will receive photon energy from sun and convert it to electrical energy.

Solar panel refers either to a photovoltaic module, a solar thermal energy panel, or a set of solar photovoltaic (PV) modules electrically connected and mounted on a supporting structure. Each module is rated by its DC output power under standard test conditions (STC). The efficiency of a module determines the area of a module given the same rated output. A photovoltaic system typically includes a panel, an inverter, a battery, and/or solar tracker, and interconnection wires (Solar panel, 2014).

Some applications of the photovoltaic system are stand-alone systems, building integrated photovoltaic system, utility power production, application of PV in the highway, etc.

Harmattan on the other hand is defined as the weather condition in West Africa during the northern winter season, where the atmospheric environment becomes ubiquitously dusty and hazy as a result of the suspension of Saharan dust floating in the northeast winds (Sunnu, 2006). The harmattan season lasts for about five months from November to March. Most countries near the Gulf of Guinea in West Africa are affected by this dusty wind phenomenon (Sunnu, 2006).

Meteorologically, the harmattan affects areas with latitudes north of the latitudinal position of the Inter-Tropical Convergence Zone (ITCZ), which separates the Saharan dustladen northeast winds from the southwest monsoon winds. The harmattan phenomenon is important to governments and scientists because of its effect on ambient air, forest canopy, global circulations, the industry, homes and offices, equipment design and performance, signal transmission, crops and plants, water surfaces, the human body, transportation and horizontal visibility (Sunnu, 2006).

Since the early 1960's, scientists noticed and studied the reduction of solar collector performance due to the dust settling on solar panel surface and they focused mainly on the thermal cells and the effects of dust accumulation on the mirror reflectance (Dietz, 1963).

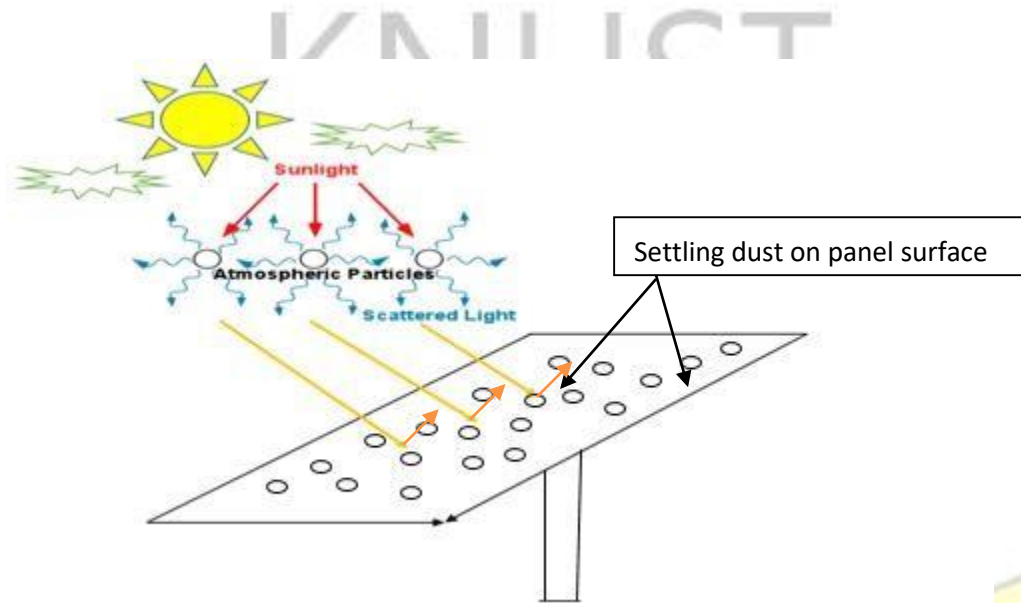


Figure 1.1 How dust affects the output of a panel

Atmospheric dust blocks sunshine radiation, scattering most fractions of the sun's rays as shown in figure 1.1. This dust further settles directly on the solar photovoltaic panels, blocking the cells from the sun's rays.

Solar photovoltaic and thermal panel's shows lower performance efficiency after a short period of time, both in electrical and thermal performance capabilities when installed in dusty conditions (Elminir, et al., 2006). Most panels are designed with the intention of operating for over two decades; however, their performance time is reduced by environmental conditions of the area, especially with settling dust.

1.2 STUDY AREA

An automatic weather station was established by Kwame Nkrumah University of Science and Technology at Walewale in the Northern region of Ghana where we experience intense harmattan dust during the dry season. It is located adjacent the Walewale government hospital.

1.3 JUSTIFICATION OF RESEARCH

Considering the above discussed impact dust has on panels, studying the degradation of the solar panels proves vital because it informs improvement of panel design and installation and also better predict the extent of performance degradation on the panels and ensure appropriate cleaning methods

1.4 OBJECTIVES

MAIN OBJECTIVE

The main objective of this thesis is to determine how harmattan dust affects the performance of photovoltaic solar panel at Walewale during the Harmattan season in Ghana.

SPECIFIC OBJECTIVES

The specific objectives of this project include;

1. To measure the environmental parameters that affect solar power output i.e. solar irradiation, temperature, dust particles and wind speed.
2. To determine the effect of atmospheric dust on the energy capture efficiency of the solar panel.
3. To determine the effect of settling dust on the current and voltage outputs of the panel.
4. To graphically model the power output module of the panel from measured data.
5. To mathematically model the effect of settling atmospheric dust particles and wind speed on the panel power output.

1.5 STRUCTURE OF THESIS

This thesis is organized into five chapters;

Chapter Two contains a literature review of solar PV systems, theory of dust, effect of harmattan dust on panel and current-voltage output.

Chapter Three presents the various methodologies considered to achieve each specific objectives.

The results and discussions of the experimental work were presented in Chapter Four.

Chapter Five contains the conclusion and recommendations of the research.

CHAPTER TWO

2.0 LITERATURE REVIEW

This chapter discusses literature on solar photovoltaic systems, production of electricity from solar panel, dust deposition, the theoretical effect of harmattan dust on solar panels and reviews of some experimental results.

2.1 SOLAR PHOTOVOLTAIC SYSTEMS

A photovoltaic system is a system which uses one or more solar panels to convert solar energy into electricity. It consists of multiple components, including the photovoltaic modules, mechanical and electrical connections and mountings and means of regulating and/or modifying the electrical output (Photovoltaic system, 2014).

The modules in a PV array are usually first connected in series to obtain the desired voltages; the individual modules are then connected in parallel to allow the system to produce more current (Photovoltaic system, 2014) as shown in figure 2.1 below.

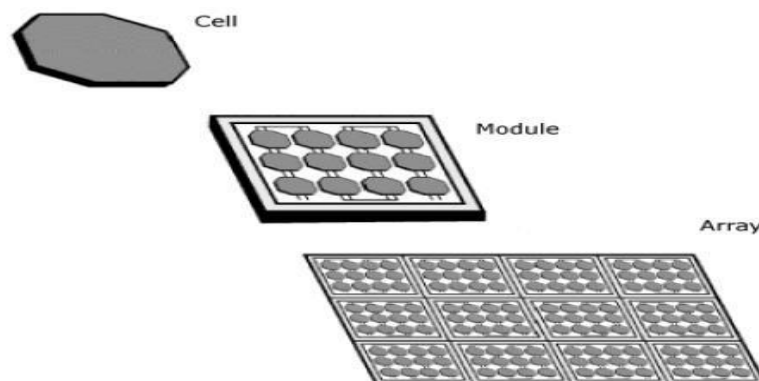


Figure.2.1. Photovoltaic system (Blueplanet-energy, 2014)

2.1.1 PHOTOVOLTAIC CELL

The solar cell is the basic unit of a photovoltaic module and it is the element in charge of transforming the sun rays or photons directly into electric power. Solar cell also called PV cell is a device that can produce a voltage difference when a source of light shines on it. When the solar cell gets connected to a circuit via wires, the electrical current flows through the wire, as a result work will be produced. French scientist Edmund Becquerel first discovered that light can be converted to electricity using some kinds of materials in 1839, later in 1876 Adams and Day noticed the selenium's photovoltaic effect. After a few years, the American Charles Frits invented the first solar cell (Goetzberger, et al., 2003). Later more advances in space programs and the 1970s energy crisis lead to more developments in the solar cell technologies. The solar cells' energy generation between 1988 and 2009, increased from 35 MW to 11.5 GW (Jager-Waldau, 2011).

There are four major types of PV cells namely, mono-crystalline (or single crystalline), poly-crystalline, amorphous and organic cells. Nano PV is also a newly introduced kind of solar cells (Razykov, et al., 2011). Solar cells are mostly produced out of copper, copper indium diselenide, gallium arsenide, etc., while its specific optical properties silicon holds the top position among these materials (Contreras, et al., 2006). Space crafts, marine navigation aids, telecommunication, cathodic protection, water pumping, remote area power supply (RAPS) systems and many others are among the various applications of PV cells (Kalogirou, et al., 2007).

2.1.2 COMPONENTS OF PV SYSTEM THAT PROVIDE ELECTRICITY

The four primary components for producing electricity using solar power, which provides common 110-120 volt AC power for daily use are: Solar panels, charge controller, battery and inverter. Solar panels charge the battery, and the charge regulator insures proper charging of the battery. The battery provides DC voltage to the inverter, and the inverter converts the DC voltage to normal AC voltage. If 220- 240 volts AC is needed, then either a transformer is added or two identical inverters are series-stacked to produce the 240 volts (PEOM, 2010).

2.2 THEORETICAL MODELLING OF SOLAR CELL

An ideal PV cell is modeled by a current source in parallel with a diode. However no solar cell is ideal and thereby shunt and series resistances are added to the model as shown in the PV cell in figure 2.2. The intrinsic series resistance, R_s has it value very small while the intrinsic shunt parallel resistance, R_{sh} has a very high value.

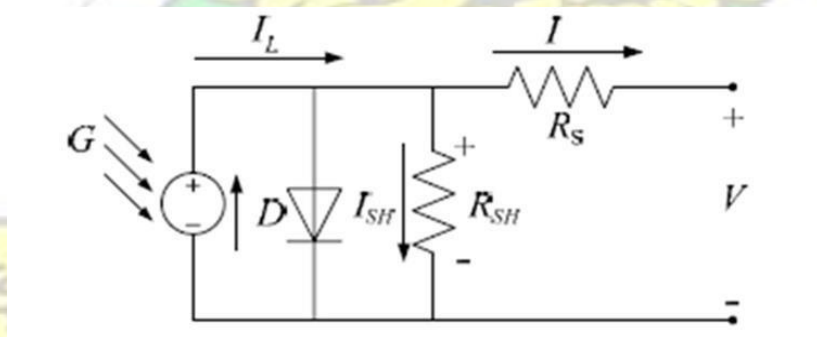


Figure.2.2. Circuit diagram of the PV model

The process of modeling this solar cell can be developed based on the net current of the cell, I defined as the difference of the photocurrent, I_L (the current generated by the incident light, directly proportional to the sun irradiation) and, I_d (the normal diode current), as shown in equation below;

$$I = I_L - I_d \quad (2.1)$$

An ideal solar cell can be represented by a current source connected in parallel with a rectifying diode, as shown in the equivalent circuit of Figure 2.3. The corresponding I-V characteristic is described by the Shockley solar cell equation (Markvart, et al., 2003)

$$I = I_L - I_0 \left(e^{\left(\frac{qV_d}{nkT} \right)} - 1 \right) \quad (2.2)$$

Where; $I_d = I_0 \left(e^{\left(\frac{qV_d}{nkT} \right)} - 1 \right)$

K = Boltzman constant = 1.38×10^{-23} J/K

T = Temperature in Kelvin q = Charge of

an electron = 1.6×10^{-19} C V_d = Diode

voltage (Volt) n = The ideality factor

Applying Kirchhoff's law to the node where I_L , diode, R_{SH} and R_S meet, we get

$$I_L = I_d + I_{SH} + I \quad (2.3)$$

Thus; $I = I_L - I_d - I_{SH}$

$$I_{SH} = \frac{V_{SH}}{R_{SH}} = \frac{V_d}{R_{SH}} = \frac{V + IR_S}{R_{SH}}$$

Hence;

$$I = I_L - I_0 \left(e^{\left(\frac{q(V + IR_S)}{nkT} \right)} - 1 \right) - \frac{V + IR_S}{R_{SH}} \quad (2.4)$$

Where; Temperature dependence of the diode saturation current, I_0 .

- Temperature dependence of the photo current, I_L .
- Series resistance, R_S , which gives a more accurate shape between the maximum power point and the open circuit voltage. This represents the internal losses due to the current flow.

- Shunt resistance, R_{sh} , in parallel with the diode, this corresponds to the leakage current to the ground and it is commonly neglected.

The assumption $I_{SC} \approx I_L$ is generally used in the modeling of PV devices because in practical devices the series resistance is low and the parallel resistance is high. The light-generated current of the PV cell depends linearly on the solar irradiation and is also influenced by the temperature according to the following equation (Marcelo, et al., 2009);

$$I_L = I_L + K_0(T - T_1) \quad (2.5)$$

Where T and T_1 , being the actual and reference temperature in Kelvin respectively, G (W/m^2) is the irradiation on the module surface, and G_n (W/m^2) is the nominal irradiation. Equations 2.2, 2.3, 2.4, 2.5 was modeled in appendix A with a matlab code

$$I_L(T_1) = I_L(T_{1,nom}) * \frac{G}{G_{nom}} \quad (2.6)$$

Cell current at various irradiance levels can be calculated by the following equation (Marcelo, et al., 2009) ;

$$I_L(G) = I_L(G_{nom}) * \frac{G}{G_{nom}} \quad (2.7)$$

Where; G irradiance level (kW/m^2), G_{nom} , is $1 kW/m^2$ at AM (Air Mass) 1.5, $I_L(G_{nom})$, cell current at G_{nom}

2.2.1 POWER OUTPUT OF CELL

The power extracted from a PV cell is the product of current and voltage.

$$P_{cell} = (I_{cell}) * (V_{cell}) \quad (2.8) \text{ The open circuit voltage is}$$

logarithmically dependent on the cell illumination level. The short circuit current also is dependent on cell illumination level (Meral ME et al, 2011).

For the maximum power produced by the solar cell, the following equation can be used.

$$P_{max} = V_{max} * \left[I_L - I_O \left(e^{\frac{q(V_{max} + I_{max} R_S)}{nkT}} - 1 \right) - \frac{V_{max} + I_{max} R_S}{R_{SH}} \right] \quad (2.9)$$

$P_{max} = (I_{max}) * (V_{max}) = (FF) * (I_{sc}) * (V_{oc})$ (2.10) FF shows the quality of solar cell (Skoplaki, et al., 2009). It is the ratio of the maximum power that can be delivered to the load and the product of I_{sc} and V_{oc}

$$FF = \frac{P_{MAX}}{I_{sc}V_{oc}} = \frac{I_{MAX}V_{MAX}}{I_{sc}V_{oc}} \quad (2.11)$$

2.2.2 EFFICIENCY OF PV CELL

The efficiency of a PV cell is defined as the ratio of peak power to input solar power.

$$\eta = \frac{V_{MP} I_{MP}}{I \left(\frac{W}{m^2} \right) A (m^2)} \quad (2.12)$$

Where, V_{mp} is the voltage at peak power, I_{mp} is the current at peak power, I is the solar intensity per square meter, A is the area on which solar radiation fall. For maximum efficiency, we track the maximum power from the PV system at different environmental condition such as solar irradiance and temperature by using different methods for maximum power point tracking.

2.2.3 STANDARD TEST CONDITIONS (STC)

The comparison between different photovoltaic cells can be done on the basis of their performance and characteristic curve. The parameters were tabulated in a datasheet.

The datasheet makes available the notable parameters regarding the characteristics and performance of PV cells with respect to standard test condition.

Standard test conditions are as follows:

$$\text{Temperature } (T_n) = 25^{\circ}\text{C}$$

$$\text{Irradiance } (G_n) = 1000 \frac{\text{W}}{\text{m}^2}$$

2.3 THEORETICAL CONSIDERATIONS OF DUST

Aerosols are two-phase systems namely the particulate phase and the fluid (normally air) phase in which the particles are suspended. The behavior of the particles within the fluid depends, to a large extent, on the motion and the intrinsic properties of the suspending fluid. Sub-micrometer particles (diameter $< 1.0 \mu\text{m}$) and normally aerosol particles with sizes approaching the mean free path of the suspending fluid are affected by the motion of the individual fluid molecules and are therefore analyzed by the kinetic theory of gases under the free molecular regime (Sunnun, 2006).

The general equation that governs the motion of particles in air (or a gas) depends upon the relative velocity between the particle and the air. The effect of the interaction between the fluid and the flowing particle produces a resisting force of the fluid on the particle in the direction of the upstream velocity. This force is termed the drag, F_D . The flow field is a function of the shape of the particle and the parameters such as particle size, orientation, speed and fluid properties. The drag force on small spherical suspended particles in a flow of low Reynolds numbers, $Re \ll 1$, is given by the Stokes law (Hinds 1999; Massey 1994)

$$F_D = 3\pi\mu DV \quad (2.13)$$

Where μ is the absolute viscosity of the fluid, D is the diameter of the particle and V is the velocity of the particle relative to the prevailing undisturbed wind speed. The Stokes law applies to flow situations where:

- i) The fluid is incompressible: there are no walls or other particles nearby, the motion of the particle is constant, the particle is a rigid sphere, and the fluid velocity at the particle's surface is zero;
- (ii) The diameter of the particle is the characteristic length and;
- (iii) The settling velocity of the particle relative to the prevailing wind velocity is the characteristic velocity.

In order to predict if a falling particle is governed by Stokes law, the particle Reynolds number, Re must be less than unity ($Re < 1$) (Hinds 1999). Re is defined as

$$Re = \frac{\rho V D}{\mu} \quad (2.14)$$

Where, ρ is the density. If the drag force given by Stokes' law and that given by Newton's law are compared we obtain the coefficient of drag, C_D that relates the drag force to the velocity pressure, and as a function of Re . This relationship between particle Reynolds number, Re , and drag coefficient C_D is therefore divided into 3 regimes for laminar flow or Stokes regime, transition flow regime (an intermediate regime) and Newton or turbulent flow regime. The relationships according to Allen (1981) are given as:

$$\begin{aligned} C_D &= 24 / Re && \text{if } Re < 0.2 \\ C_D &= 24 / Re (1 + 0.3 Re), && 0.2 < Re < 2.0 \\ C_D &= \frac{24 (1 + 0.15 Re^{0.687})}{Re} && 2 \leq Re < 700 \end{aligned} \quad (2.15)$$

Stokes equation may therefore be used for low Reynolds numbers, ($Re < 0.2$) to determine the settling velocity of particles flowing in the atmosphere. When the characteristics of the settling particles diverge farther from the stated assumptions, corrections may be applied to determine the actual settling behaviour such as for non-spherical particles and very small particles ($D < 1 \mu m$), which cause non-zero velocity at the particle surface. The equation for drag and settling velocity are based on spherical particles. However, most solid particles are non-spherical such as cubic (for sea salt particle), cylindrical (bacteria and fibres), single crystals, clusters of spheres, agglomerated particles or crushed materials, which have irregular shapes. The shape of a particle affects its drag force and settling velocity. A usual form of the settling velocity of a suspending particle of density ρ_p is given as (Hinds 1999);

$$V_s = \frac{1}{18} \frac{D^2 \rho_p g C_c}{\mu} \quad (2.16)$$

Where, C_c is the Cunningham slip correction factor, which for small particles whose size approaches the mean free path, (λ) of the suspending gas is given as (Hinds 1999)

$$C_c = \frac{2.52}{D} \lambda$$

Where, C_c is significant for particles less than $1 \mu m$ in diameter.

2.4 DUST DEPOSITION

The deposition of an aerosol particle is the result of two kinds of forces namely a constant external force such as gravity and the resistance of the air to particle motion. Analysis of these forces is important in determining the deposition flux of the aerosols in the following section.

2.4.1 FACTORS AFFECTING DUST SETTLEMENT ON PV PANEL

The characteristics of dust settlement on PV systems are influenced by the property of dust and the panel surface properties. The property of dust (type – chemical, biological and electrostatic property, size, shape and weight), is as important as its accumulation/aggregation. Likewise, the surface finish of the settling surface (PV) also matters. A sticky surface (furry, rough, adhesive residues, electrostatic buildup) is more likely to accumulate dust than a less sticky, smoother one. It is well-known that dust promotes dust, i.e. with the initial onset of dust, it would tend to attract or promote further settlement onto the surface becoming more amenable to dust collection (Mani and Pillai, 2010).

Taking into account the effect of gravity, horizontal surfaces usually tend to accumulate more dust than inclined ones. This however is dependent on the prevalent wind movements (Speed and direction). Generally a low-speed wind pattern promotes dust settlement while a high-speed wind regime would on the contrary, dispel dust settlement (Mani and Pillai, 2010). However, the geometry of the PV system in relation to the direction of wind movements can either increase/decrease the prospects of dust settlement at specific locations of the PV system. Dust is likely to settle in regions of low-pressure induced by high-speed wind movements over inclined/vertical surface. The dispersal of dust attributed to wind movements and geometry of PV system depends on the property of dust (weight, size, type) (Mani and Pillai, 2010).

A framework to understand the various factors that govern the settling/assimilation of dust is illustrated in Fig. 3.4. It is easy to discern that the phenomenon of dust settlement is extremely complex and challenging to practically handle/comprehend given all the factors that influence dust settlement. PV installations are generally expected to be designed

for optimum yield or output (Mani and Pillai, 2010). The factors that determine optimum or maximum yield can be categorized into those that are alterable and those that remain unalterable. The factors that can be altered provide design flexibility to respond to varying installation requirements; the factors that are unalterable need to be accommodated by default. The various alterable and unalterable factors that influence the design, installation and operation (and maintenance) of PV systems is illustrated in figure. 2.3.

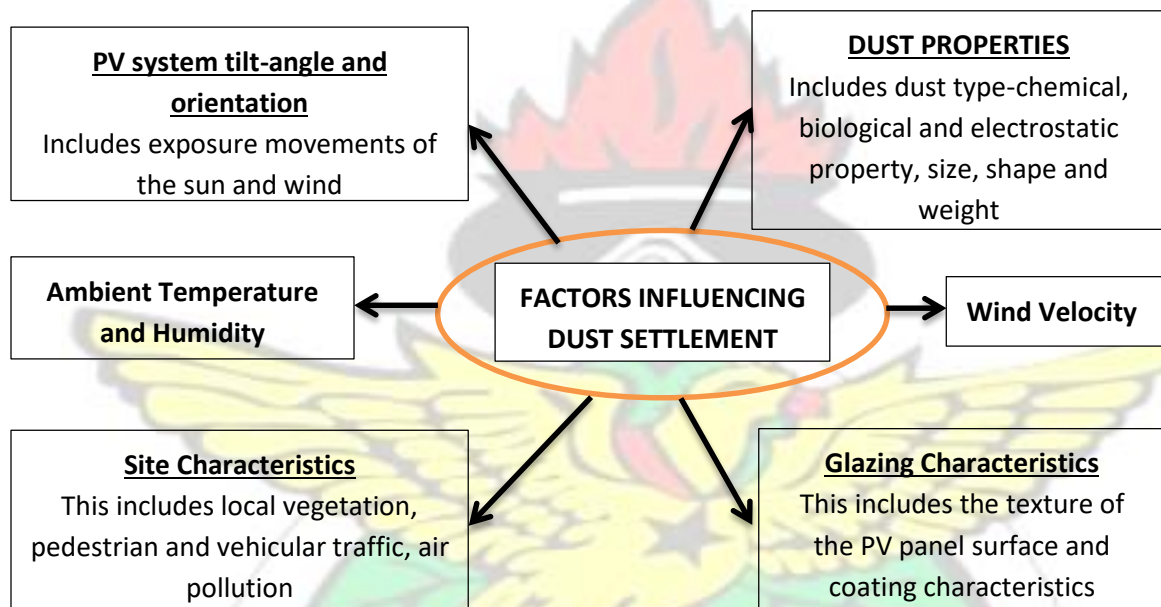


Figure.2.3. Factors affecting dust settlement

2.4.2 MECHANISM OF DUST DEPOSITION

Deposition is the major process of dust removal from the atmosphere. Dust deposition on surface depends on the various factors such as dust concentration in the air, wind velocity, surface shape, particle size, settling velocity of particle and atmospheric moisture (Pye, 1989). The crucial mechanism leading to dust deposition is the

sedimentation due to gravity according to Stokes law. As a result of this process large particles sediment out more quickly than smaller ones. (Mahowald, et al., 2005). The following are some mechanisms of dust deposition and their corresponding definitions:

I. Gravitational settling (sedimentation): Particles are removed from the atmosphere due to gravitational force. Gravitational settling is the prevailing process for large particles which have diameter more than 5 μm . For such particles a settling velocity is a suitable physical and easily measured quantity.

II. Inertial Impaction and Interception: As a result of inertia, a particle moving in a streamline can strike with slowly moving or stationary obstacles (targets) along its path. As the streamline deflects around the obstacle, the particle continues its motion toward the object and impacts it. The probability of occurrence of an impaction is mainly affected by aerodynamic particle size and the relative velocity between the particle and the obstacle (or target). Bigger particles are collected more easily than smaller particles due to their greater inertia. Furthermore, collection efficiency increases as the relative velocity between the particle in the streamline and the obstacle (or target) increases.

III. Brownian motion: This is the process by which aerosol particles move randomly due to collisions with gas molecules. Such collisions may lead to further collisions with either obstacles or surfaces.

Dust deposition is the third phase of wind erosion. Dust emission generated by wind erosion is the main source which affects the atmospheric radiation balance in direct methods (through scattering and absorbing various radiation components) as well as indirect methods (through modifying the optical properties and lifetime of clouds). Wind erosion is a complex process governed by numerous factors that can be classified as: atmospheric conditions (e.g. wind, precipitation and temperature), soil properties (soil

texture and composition), land-surface characteristics (e.g. topography, moisture and aerodynamic length) and land-use practices (e.g. farming, grazing and mining). The physics of wind erosion is complex and is so far not fully understood. Wind erosion has three distinct phases namely: 1- particle entrainment (by aerodynamic lift, disaggregation), 2- transport and 3- deposition (dry and wet deposition) (Shao, 2008).

There are two fluxes that result in a net dust accumulation, namely: dust deposition and dust resuspension. Dust deposition is the settling of particles in air on a certain surface and is characterized by an overall deposition velocity. Resuspension is the removal of the accumulated dust from the surface back to the air. To remove a dust particle from the surface, a force is needed to counteract the adhesion force between the dust and the surface.

2.4.3 STOKES'S SETTLING

Stokes terminal settling velocity of spherical particles is the velocity of the particle when the net gravitational force acting on the particle and the viscous drag exerted by the fluid are balanced. One important application of the Stoke's law is the determination of the velocity of an aerosol particle undergoing gravitational settling in still air. The harmattan period is marked by suspension and deposition of fine dust carried by the trade winds. Thus, the principle of deposition of the dust particles is generally by dry gravitational settling. Therefore the Stokes law, which applies to the settling of small particles, can be used for the deposition of the dust particles.

When a particle is released in air it quickly reaches its terminal settling velocity, a condition of constant velocity where the drag force and buoyancy force is equal and opposite to the force of gravity. Another assumption is that the presence of the aerosol

particles does not change the structure of the carrier fluid, and then Stokes law is applicable to the settling of the particles. In order to find the expression for the terminal settling velocity, w , consider a spherical particle of diameter Dp , density, ρ_p in a fluid of density, ρ_a as shown in the figure. 2.4 below;

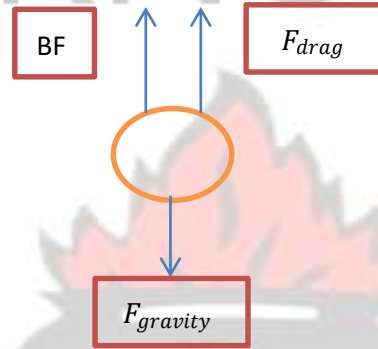


Figure 2.4. Free body diagram of a spherical particle in a viscous fluid (air)

When the spherical particle is at equilibrium, then the vector sum of upward and downward forces acting on the particle will be zero. This is mathematically expressed as

$$B_F + F_D = F_G \quad (2.17)$$

Where, B_F is the buoyancy of the surrounding air given as;

$$B_F = \frac{\pi}{6} \rho_a g Dp^3 \quad (2.18)$$

F_D is the aerodynamic drag on the particle given by Stokes law as

$$F_D = 3 \pi \mu w Dp \quad (2.19)$$

F_G is the gravity force or weight of the particle, given as

$$F_G = \frac{\pi}{6} \rho_p g Dp^3 \quad (2.20)$$

w , is the settling velocity of particles relative to the wind velocity. All other forces including electrostatic forces are neglected, Substituting (3.18), (3.19) and (3.20) into (3.17) and solving gives;

$$\frac{\pi}{6} \rho_a g Dp^3 + 3 \pi \mu w Dp = \frac{\pi}{6} \rho_p g Dp^3 \quad (2.21)$$

$$V_g = \frac{(\rho_p - \rho_a)gDp^2}{18\mu} \quad (2.22)$$

If we neglect the air density relative to the particle density, the settling velocity is given as:

$$V_g = \frac{(\rho_p)gDp^2}{18\mu} \quad (2.23)$$

The settling velocity of particles in a fluid of infinite extent is widely used to determine the size of the particle, which is proportional to the square root of the settling velocity. From equation (3.14), it can be seen that the settling velocity increases rapidly with particle size, being proportional to the square of the particle diameter. The mass concentration is computed by assuming the dust particle as a spherical shape. The mass of a particle with

density ρ was obtained as $m = \frac{\pi}{6} \rho D^3$.

2.4.4 ADHESION OF DUST PARTICLE

Great abundance of dust particles is present all around us in the atmosphere especially in the harmattan season. Dust particles are created by several ways including mechanical abrasion, chemical reactions, and combustion processes. They are known to have a very serious effect on the performance of solar collectors and are among major yield loss factor (Bowling, 1988). These particles adhere to surfaces with great tenacity.

Understanding of particle adhesion mechanism is vital to search for means to insure the particle free surfaces and effective particle prevention from depositing on the surface. Modeling physical adhesion is complex due to the fact that adhesion force is a combination of physical and chemical forces, as well as mechanical strains and stresses, all at and around that adhesion interface. Furthermore, adhesive forces can only be measured destructively

and its measurement, therefore, does not necessarily represent an equilibrium situation; hence a kinetic model of adhesion is required (Bowling, 1988).

Interactions between solids which result in adhesion can be classified into several groups. The first group includes long-range attractive interactions, such as van der Waals force, image force, gravity force and magnetic attraction, which act to place the particle down to the surface and set up the adhesion contact area. The second group contains other forces which, along with the first group of forces, institute the adhesion area. The third group involves very short range interactions which can add to adhesion only after the establishment of an adhesion contact area. These include chemical bonds of all types and intermediate bonds such as hydrogen bonds (Krupp, et al., 1967). Gravity force predominates for large particles while van der Waals forces predominate for smaller particles. Therefore, the minimum removal force must be predominant over adhesive force and weight of the dust particle in order for the particle to be detached from the surface. Mathematically this is written as;

$$F_{removal} > F_{gravity} + F_{adhesion}$$

Inversion of solid surfaces with adhering dust indicates that the gravitational force fails to overcome the adhesion force of most particles.

ADHESIVE FORCE BETWEEN A SPHERICAL PARTICLE AND A FLAT SURFACE

Considering of adhesion force between ideally flat surface and a small spherical particle resting on it shown in figure. 2.5;

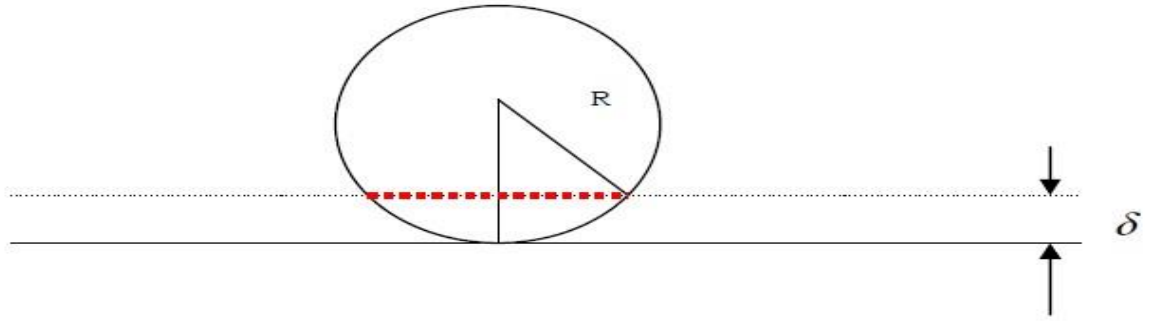


Figure.2.5. Spherical particle rests on ideally flat surface

R denotes the radius of the sphere and δ , the typical (effective) ranges of influence of short range adhesive forces between these surfaces. Hence the adhesive contact area is

mathematically expressed as;

$$S_{con} = \pi r^2 = \pi (R^2 - (R - \delta)^2) \quad (2.24)$$

Simplifying this we arrive at

$$S_{con} = \pi d (2R - \delta)$$

Where S_{con} , is Surface contact,

Therefore, the adhesive force is;

$$F_{adh} = S_{con} * U_t \quad (2.25)$$

Substituting we find;

$$F_{adh} = \pi d (2R - \delta) * U_t \quad (2.26)$$

Where, U_t is pressure in units of dyne per squared centimeter. ($1 \text{ dyn/cm}^2 = 10^{-6} \text{ bar}$)

Deposited dust strongly adheres to solar panels and solar concentrators and obscures the solar radiation reaching the PV cells and mirrors, reducing energy conversion significantly (Malay, 2013).

2.5 EFFECT OF DUST ON PV CELL PERFORMANCE

Dust is defined as the minute solid particles with less than 500 μm in diameter. Dust settlement mainly relies on the dust properties (chemical properties, size, shape, etc.) as well as on the environmental conditions (site-specific factors, environmental features and weather conditions). The surface finish, tilt angle, humidity and wind speed also affect dust settlement on the panel surface (Mani and Pillai, 2010). There have been different studies conducted to investigate the effect of dust on solar cells. Hottel and Woertz (1942) did a similar work when they stated that a wide range of reduction in performance of panel have been reported including average reduction of 1% with a peak of 4.7% in a two-month period in United States, 40% degradation. Mani and Pillai (2010) also reported from their experimental results that in a 6-month period in Saudi Arabia, there was 32% reduction in power due to the effect of dust and in 8-month time, a 17%–65% reduction depending on the tilt angle in 38 days in Kuwait. Shaharin, et al. (2011) concluded that reduction in the peak power generated by the panel can be up to 18% in Malaysia not specifying the duration of data collection. It was also shown that under greater irradiation, the effect of dust became slightly reduced but not negligible.

In another study done in Egypt, by Al-Hassan, 1998, there was a 33.5% – 65.8% reduction in performance of solar panels in duration of one to six months exposure respectively and more specifically in the tropical climate of Thailand, 11% reduction in transmittance for a period of one month was also reported. Al-Hassan (1998) concluded from the results that panels tilted with larger angles has less dust accumulating on its surface, thus less transmittance drop. As the wind speed increases, more dust deposition will occur while the dust deposition relative to the ground decreases (Goossens and

Kerschaever, 1999). Excessive dust accumulation results in deterioration of solar cell's quality and fill factor. Dust promotes dust, so that the performance of PV modules declines exponentially with more dust piling up. High humidity also helps formation of dew on the solar cell surface leading to more facile dust coagulation (Mani and Pillai, 2010).

From literature, the authors did not consider simulating the effect of air velocity on atmospheric and settled dust and its corresponding power output. The two primary ways that dust affects the photovoltaic panels were considered;

i) First, atmospheric dust blocks sunshine radiation, deflecting most fractions of the sun's rays before it reaches the panel (Al-Hasan, 1998) and also high atmospheric concentration of pollutants arising from harmattan and industrial factors causes the amount of radiation that reaches the panels to decrease resulting decrease of the solar collector quality (Goossens and Kerschaever 1999).

ii) Dust further settles directly on the solar photovoltaic panels, blocking the cells from the sun's rays. The tracing sensor of a variable angled solar panel used may be covered by dust, inhibiting the panel from tracing the sun's direction.

When there is a loss of illumination intensity caused by obscuration of light by settling dust, there are three adverse effects: (1) Reduction in power output (2) Decrease in overall efficiency (3) Formation of hotspots and dead cells if the modules are partially blocked by dust layer deposits (Rajiv, et al., 2012). When some of the cells are covered by dust, the shaded cells do not generate enough power to match the other cells; rather, they act as dead load on the working cells. As a result, the temperature of the shaded cell increases forming hotspots (Rajiv, et al., 2012). Unless efficient protection devices like bypass diodes are used to prevent the formation of hotspots, the modules can get permanently damaged (Shao, 2008).

2.6 EFFECT OF DUST ON THE I-V OUTPUTS OF A PANEL

In instances when the panel is not washed periodically, gradual accumulation of dust called edge shading can completely block small segments of the lower cells resulting in total blockage of electric current flow. Since solar cells within the PV modules are connected in series, blockage of a single cell can render a solar module totally dysfunctional. In turn, since solar strings are configured from tandem interconnection of series of solar modules, a serious case of edge shading depending on the location of a single panel can obstruct current flow through the entire string (Gevorkian, 2012).

Experiment conducted on solar cell dusting reported in the *Journal of Basic and Applied Scientific Research* by Ibrahim, 2010 (Gevorkian, 2010) indicates that solar PV module short circuit current I_{sc} can substantially degrade power output by dust accumulation while the open circuit voltage, V_{oc} is independent of dust accumulation

CHAPTER THREE

3.0 METHODOLOGY

This chapter seeks to discuss the methodological processes in achieving my specific objectives.

3.1 OBJECTIVE 1

To measure environmental parameters that affect solar power output: solar irradiation, temperature, dust particles and wind speed.

3.1.1 METHODOLOGY

An Automatic Weather Station (AWS) was procured and delivered to KNUST by Sutron Corporation. The purpose of this station was to provide information for the data collection platform (DCP) and the Dust Monitor System. The station as shown in figure 3.1 was installed and equipped with the following sensors to measure the above mentioned environmental factors;

1. Temperature sensor
2. Wind Sensor
3. Pyranometer Sensors
4. Dust Monitor Sensor
5. Data collection platform (DCP)
6. Photovoltaic system (Solar panel, charger controller, battery and invertor)



Figure.3.1. The Automatic Weather Station at Walewale.



Figure 3.2 The dust monitor sensor (ES-642)

3.1.2 FIELD MEASUREMENTS

AIR TEMPERATURE (AT) & RELATIVE HUMIDITY (RH)

Sutron's 5600-0316-1 is a high accuracy AT/RH sensor. The 5100-0021-1C radiation shield is also supplied with integrated mounting. The sensor gives two separate outputs of 0 to 1 Volt for the Air Temperature and Humidity.

Accuracy and Stability: Humidity measurement from the sensor is processed digitally, providing more scope and greater flexibility when compensating sensor characteristics such as linearity and temperature coefficient. With digital technology, the capacitive humidity sensor performance is highly precise and stable. It has an internal digital signal resolution of up to 0.03% RH and 0.03°C AT.

WIND SPEED & WIND DIRECTION

Sutron's Met-Set (sensor) uses a three cup anemometer, for accuracy, sensitivity, and durability during measurement. The cups are connected to a shaft, which turns a sensing element that converts the rotation into a series of electronic pulses. The lightweight vane tail provides the motive power for the wind direction portion of the sensor. As the vane tail moves it turns a shaft on a pair of bearings. That shaft turns a sensing element that converts the rotation into analog voltage.

GLOBAL HORIZONTAL IRRADIANCE (GHI)

CMP 11 (sensor) uses a detector design with temperature compensation. It is a step up in performance from CMP 6 and particularly suitable for upgrading meteorological networks. The faster response time meets the requirements for solar energy research and development applications. CMP 11 is also ideal for use in sun tracker based solar

monitoring stations. Two Pyranometer were provided. One measures the diffuse solar irradiance and the other, the global solar irradiance. The global solar radiation is the total irradiance falling on the panel surface ($\text{Diffuse} + \text{Direct} \cdot \cos \alpha$).

iv) DUST MONITOR SENSOR

The ES-642 as shown in figure 3.2 is a type of nephelometer which automatically measures real-time airborne TSP (total solid particles) concentration levels using the principle of forward laser light scatter phenomenon. With this phenomenon, sample air is drawn into the ES-642 by an internal diaphragm pump at a flow rate of 2 l/min. to accurately determine the sampled volume. It has a measurement Sensitivity of 0.001 mg/m³, nephelometer Accuracy of $\pm 5\%$, particle size sensitivity from 0.1 to 100 micron.

Forward Laser Light Scatter Phenomenon

The sampled air is drawn through the MD laser optical module, where an internal visible laser diode beam is collimated and directed through the sample air stream as shown in figure 3.3. The particulate in the sample air stream scatters the laser light through reflective and refractive properties. This scattered light is collected onto a silicon photodiode detector at a near-forward angle, and the resulting electronic signal is processed to determine a continuous, real-time measurement of airborne particulate mass (KNUST ES642 Manual).

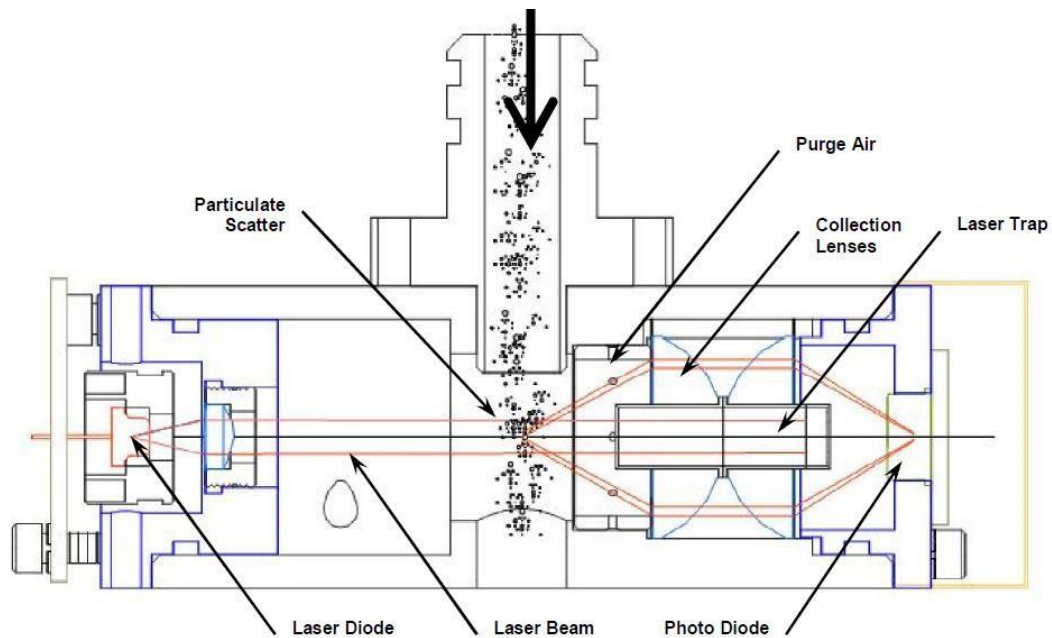


Figure 3.3 Forward Laser Light Scatter Nephelometer System

The ES-642 will output the amount of particulate in the air known as TSP (Total Suspended Particulate) in mg/m^3 . The unit normally outputs its measurement once per second by default when it is in operation. This output can be disabled by setting the Output Interval to 0. The Sensor is schedule to take sample every 45 minutes and then the data logger will collect the record this data every hour onto a flash memory.

DUST SAMPLING METHOD BY DUST SENSOR

The flow control system is an integral component of the ES-642 (Dust monitor). The diagrammatical representation of the flow system is shown in figure. 3.4. A complete description of how the instrument works is discussed below;

- i. Ambient air is drawn in through the TSP inlet at 2.0 l/m. This flow rate is used because the cut-point of the cyclones is dependent on the velocity of the particles and is only accurate at the rated flow rate.
- ii. The sample air goes through the vertical inlet tube, which is heated to keep the sample air humidity below 50% RH to prevent measurement errors caused by moisture.
- iii. The sample air stream immediately enters the laser optical module where it passes through the laser beam and the particulate is measured.
- iv. The pump filter removes any particles larger than 10 μm in diameter to protect the flow sensor and pump. The air stream then passes through the flow meter which measures the mass flow rate of the sample air as an analog electronic signal which is sent to the CPU where the ambient temperature and pressure are used to calculate the actual flow.
- v. Down-stream of the flow meter, a pulsation chamber is used to reduce the pressure pulsations caused by the diaphragm pump, which would otherwise appear as noise in the flow sensor signal. There is nothing inside the pulsation chamber.
- vi. The air is drawn into the vacuum side of the main sample pump. This is a brushless diaphragm pump which is pulse-width modulated (PWM) by the CPU to control the flow rate.
- vii. Most of the sample air exhausts through the pump to the exhaust hole on the bottom of the ES-642. A small amount (about 10%) of the pump exhaust is recirculated through a simple purge adjust valve (a screw installed in one of the ports). This

purge adjust is factory-set to control the ratio of the purge air, and should not be tampered with.

- viii. The purge air passes through the purge filter which removes any remaining particles larger than 0.2 microns in diameter. The purge air enters the laser optical module in a ring around the detector lenses, and through a port in front of the laser focus lens. The clean air circulating past the lenses greatly reduces the amount of dirty sample air which would otherwise contact and contaminate the optics.
- ix. During the zero portion of the automatic periodic self-test cycle, the main sample pump is turned off and the purge pump is turned on. The air is filtered by the purge filter and circulated through the laser module at a higher flow rate. The air in the laser module is 100% filtered during this process, and no scattered light should enter the detector. The ES-642 takes a zero reading and establishes a new signal baseline. A check valve prevents air from back-flowing through the purge pump during normal sampling.

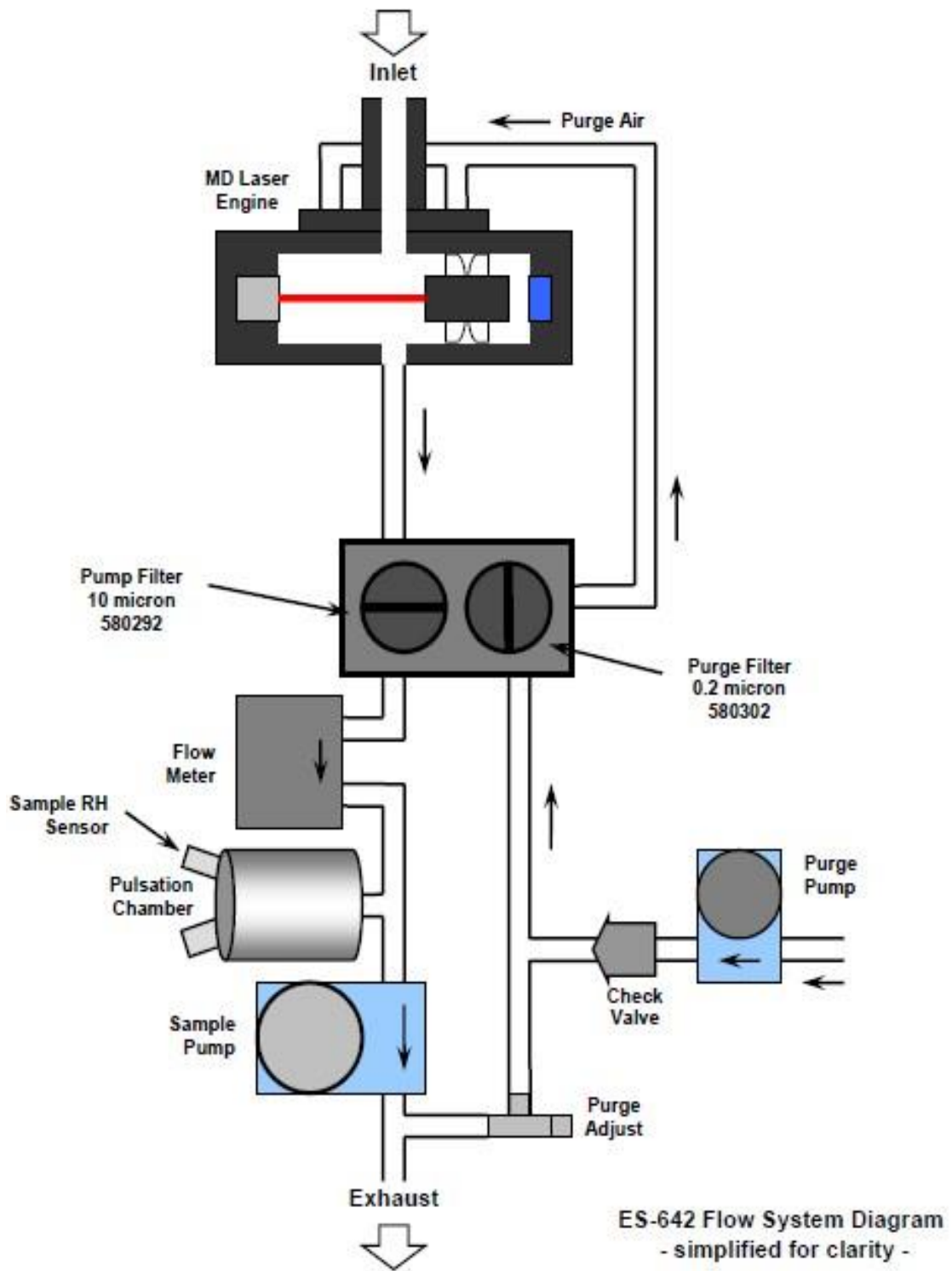


Figure.3.4. ES-642 Airflow System Diagram (Source: KNUST ES642 Manual)

3.1.3 SENSOR'S CONFIGURATION

The 9210 data logger automatically samples, measures and logs the sensors' data as per details given in the AWS Setup configuration section and log the data in its flash memory. The configuration of the AWS station was based on the sensor measurement scenario. Each sensor required an average value for an hour sampling measurement. Table 3.1 shows the measurement intervals for each parameter with their respective sensor. These intervals were configured in the 9210 XLite.

Table 3.1 Configuration of the installed sensors at the weather station

Parameter	Tag Name	Interval	Units
Air Temperature AVG	AT	1:00:00	C
Relative Humidity AVG	RH	1:00:00	%
Wind Speed AVG	WS	1:00:00	m/s
Wind Direction AVG	WD	1:00:00	Deg
Global Horizontal Irradiance	GHI1HR	1:00:00	W/m ²
Total Suspended Particulate	TSP	1:00:00	mg.m ³

3.1.4 PHOTOVOLTAIC SYSTEM

The photovoltaic system consist of the four components involved in producing electricity as shown in figure 3.5. These components are; the solar panel, charge controller, battery and an inverter.

SOLAR PANEL

The panel (Number BSP 50-12) was manufactured by Power-up Company limited, Maryland. Data were taken during the harmattan season from November, 2014 to February, 2015.

General Information on Panel;

1. High performance mono multi-crystalline cells.
2. High energy yields in a wide variety of climates.
3. Anodized aluminum frame provides for easy mounting.

The physical and electrical characteristics of the panel are stated in Table 3.2 and 3.3.

Table 3.2. The Physical characteristics of the panel

Length	(Inches) mm	(33) 839
Width	(Inches) mm	(21.125) 537
Thickness	(Inches) mm	(1.33) 34

Table 3.3. The Electrical Characteristics of the panel

Rated Power	Pr	50 W
Peak Power	Pmpp	50.9 W
Peak Power Voltage	Vmpp	17.03 V
Peak Power Current	Impp	2.99 A
Open Circuit Voltage	Voc	21.02 V
Short Circuit Current	Isc	3.62 A

$$\text{Cell area} = 839\text{mm} * 537\text{mm} = 450543 \text{ mm}^2 = 0.451 \text{ m}^2.$$

Electrical efficiency = 14% with a power peak of 50 W.

Number of cells = $4 \times 9 = 36$ cells

The performance of the solar panel is measured at standard test conditions (STC) of 1000 W/m² irradiance, AM 1.5, and at 25 °C cell temperature.

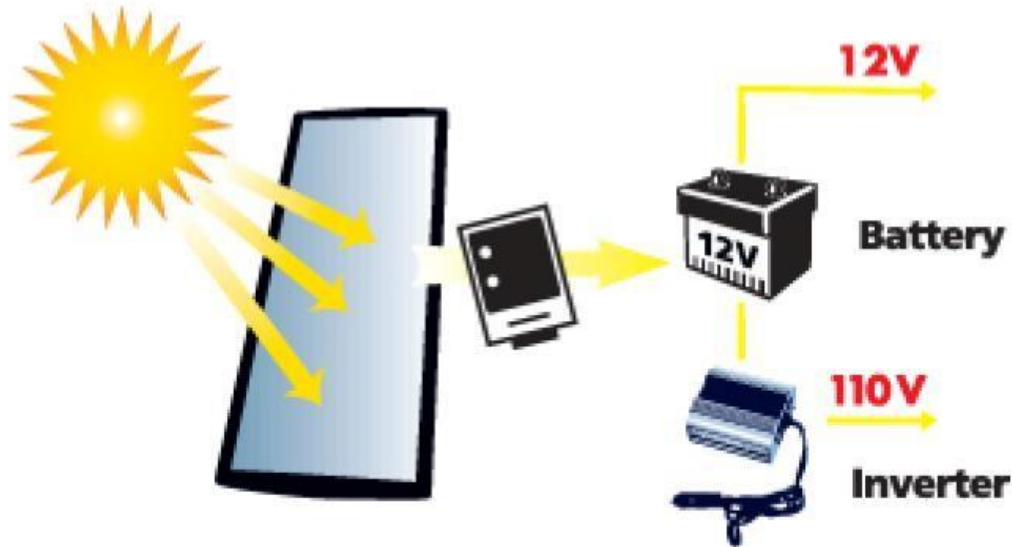


Figure 3.5. The photovoltaic system (Photovoltaic system, 2014)

CHARGE CONTROLLER

A charge controller monitors the battery's state-of-charge to insure that when the battery needs charge-current it gets it, and also insures the battery isn't overcharged. Connecting a solar panel to a battery without a regulator seriously risks damaging the battery and potentially causing a safety concern.

BATTERY

Lead-acid batteries was considered as they are commonly in PV systems because it cost less and are readily available nearly everywhere in the world. Lead-acid batteries are available in both wet-cell (requires maintenance) and sealed no-maintenance versions. The size of the battery bank required will depend on the storage capacity required, the maximum

discharge rate, the maximum charge rate, and the minimum temperature at which the batteries will be used. During planning, all of these factors were considered, the size of the battery used in this this project was 12 V

INVERTER

An inverter is a device which changes DC power stored in a battery to standard 120/240 (Voltage Alternating Current) VAC electricity (also referred to as 110/220). Most solar power systems generate DC current which is stored in batteries. Nearly all lighting, appliances, motors, etc., are designed to use ac power, so it takes an inverter to make the switch from battery-stored DC to standard power (120 VAC, 60 Hz).

3.2 OBJECTIVE 2 and OBJECTIVE 3

Objective 2: To determine the effect of atmospheric dust on the energy capture efficiency of the solar panel.

Objective 3: To determine the effect of settled dust on the current and voltage outputs of the panel.

3.2.1 METHODOLOGY

The measured values of atmospheric dust, voltage of the panel was tabulated and analysed. The data collection platform (DCP) did not record the values of current and efficiency. The current output of the panel was modelled in mat-lab in appendix A with the voltage, radiation and panel temperature. Among these influential parameters, dust affected directly the sun radiation by scattering in the atmosphere and blocking sun rays when they deposits on the panel surface. Radiation is a linear function of the current output of the

panel, thus changing values (increase or decrease) of radiation resulted in a linear increase and decrease in panel current output.

At a given radiation, voltage and current output, the panel efficiency was derived from the equation

$$\eta = \frac{V * I}{R\left(\frac{W}{m^2}\right) * A(m^2)} \quad (3.1)$$

Where, V is the voltage at peak power, I is the current at peak power, R is the solar intensity per square meter, A is the area of the panel.

The influence of dust on panel efficiency, current and voltage values was graphically represented and further discussions were made in chapter 4.

3.3 OBJECTIVE 5

To model the effect of settling atmospheric dust particles and wind speed on the panel power output

3.4.1 METHODOLOGY

Data collected on the dust monitor and wind gauge during the period of studies was analyzed to determine how this parameters affects the panel power output. The instruments were configured to measure or sample an average hourly data during the period of studies.

The experimental site is located at 10°21'N latitude and 0°48'W longitude and at altitude approximately 166 m (above sea level). The average temperatures during this season vary between 10°C at night and a maximum of about 45°C during the day. There is formation of dew in the early morning and the late evening due to considerable temperature difference in the day and night. The dew deposited on the surface acts as glue to adhere the

dust particle more to the surface. Wind velocity at lower speeds reduces the efficiency of the module due to high deposition of dust on panel surface while at higher velocities they are carried out of dust layers away from panel surface by convective wind transport means but the attachment between particle and surface becomes much stronger when dew evaporates. The strength of attachment increases as the process continues (i.e. when more dew deposited on the surface and evaporated).

Dust deposition on a surface illustrated in figure 3.6, is also defined as a function of the environment and surface conditions and the type of particles.

$$dust_{deposited} = f_1(\text{air flow, surface condition, type of particles, other forces})$$

$$dust_{resuspended}$$

$$= f_2(\text{air flow, surface condition, particle type, dust load, other forces})$$

Where;

$$dust_{deposited} = \text{rate of settling particles on the surface (mg/m}^2\text{/h),}$$

$$dust_{resuspended} = \text{rate of removal of particles from the surface (mg/m}^2\text{/h).}$$

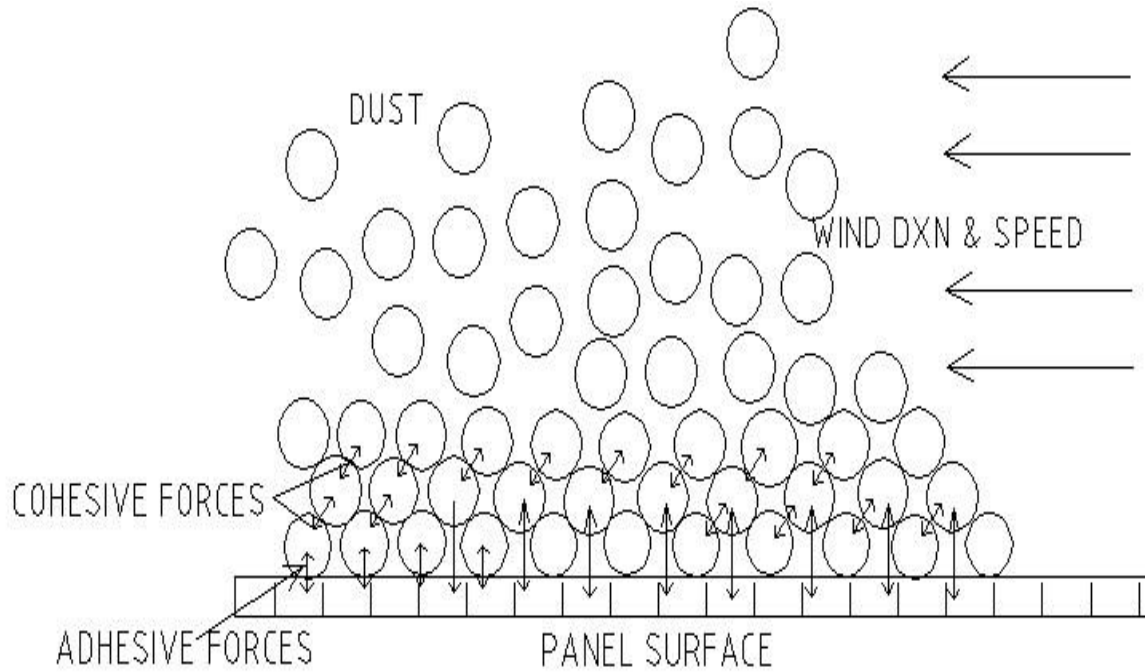


Figure.3.6 Interactions between dust and panel surface and itself

In a first step, deposition and resuspension are not analyzed individually but combined, and the net deposition rate is:

$$\Delta_{dust} = dust_{deposited} - dust_{resuspended} \quad (3.2)$$

$$dust\ load = \int \Delta_{dust} dt + initial\ dust\ load \quad (3.3)$$

Where; Δ_{dust} = rate of change of the dust load ($mg/m^2/h$), dust load = amount of particles on the surface per unit area ($mg/m^2/h$), t = time (h).

The resuspension rate is supposed to be constant versus time; at least until the dust load reaches a certain level since the deposition is also constant and according to equation (3.18) the dust load is directly proportional to time up to this level.

The duration of the experiment reaches a critical time where the dust load is no longer proportional to time i.e. the point maximum load of dust deposition because of less adhesive

force between particles in further layers from the panel surface. And it is also assumed that the deposition is proportional to the airborne concentration but independent of time. Hence, Δ_{dust} is not dependent on time after a long period and equation (3.2) can be integrated and solved for Δ_{dust} . The integration constant is zero because the initial dust load is also zero.

$$\Delta_{dust} = \frac{\text{dust load}}{t} \quad (3.4)$$

3.4.2 MATHEMATICAL MODULE

The objective under consideration sought to develop a mathematical module from the measured data of settling dust, wind and power output to analyze the relationship and dependence of this variables with each other.

These methods were considered in my module

1. LINEAR REGRESSION BY METHOD OF LEAST SQUARES FOR THREE VARIABLES
2. LINEAR REGRESSION METHOD WITH MATHEMATICAL MODEL SOFTWARE (R and mat-lab)

With linear regression, problems involving more than two variables can be treated in a manner analogous to that for two variables. A relationship among these three variables P, V, D can be described by the equation

$$P = a_0 + a_1D + a_2V \quad (3.5)$$

Which is called a linear equation in the variables P, V, D

METHOD OF LEAST SQUARE FOR THREE VARIABLES

$$\begin{aligned}\sum P &= Na_0 + a_1 \sum D + a_2 \sum V \\ \sum PD &= a_0 \sum D + a_1 \sum D^2 + a_2 \sum DV \\ \sum VP &= a_0 \sum V + a_1 \sum DV + a_2 \sum V^2\end{aligned}$$

Where P, V, D are Power output, Wind velocity and Settling dust respectively. N, is the number of data collected and a_0 , a_1 , a_2 are coefficient.

Mathematical software's used were R and Mat-lab to also module for the mathematical relationship between the variables power output, wind velocity and dust sampled. A mathematical code was written after studying the data of the parameters under consideration and the developed equation from the code was compared to the measured data from the weather station.

CHAPTER FOUR

4.0 RESULTS AND DISCUSSION

This chapter focuses on the analysis and interpretation of experimental data. It further discusses the relationship between variable parameters and its influence on others.

4.1 OBJECTIVE 1

To measure environmental parameters that affect solar power output: solar irradiation, temperature, dust particles and wind speed.

4.1.1 RESULTS AND DISCUSSION

The data collected from the measuring instruments used during my period of studies, from 1st November, 2014 to 28 Feb, 2015 (120 days) is clearly tabulated in table 4.1. The wind velocity was measured at a height of 2 meters. The solar panel was 3.5 meters from the ground surface.

Table 4.1 Tabulated experimental data

Days	Total Dust Particle (mg/m ³)	Dust Deposited (mg/m ²)	Atmospheric Temp. (C)	Wind Velocity (m/s ²)	Average Radiation (W/m ²)
1	0.274	0.073	30.83	2.00	313.45
2	0.368	0.098	31.11	2.40	238.00
3	0.478	0.127	32.40	2.30	284.63
4	0.456	0.121	32.55	2.32	274.88
5	0.174	0.046	27.25	1.50	141.66
6	0.235	0.063	26.19	1.40	302.00
7	0.416	0.111	32.77	2.41	300.15
8	0.810	0.216	33.28	2.48	278.59

Table 4.1 continued. Tabulated experimental data					
9	0.552	0.147	33.55	2.50	286.80
10	0.516	0.137	32.93	2.43	282.11
11	0.393	0.105	31.54	2.50	247.45
12	0.223	0.059	30.54	2.20	227.94
13	0.244	0.065	28.57	1.50	289.25
14	0.364	0.097	31.57	2.02	282.03
15	0.546	0.145	31.57	2.00	300.63
16	0.548	0.146	32.80	2.30	303.06
17	0.423	0.113	31.79	2.31	264.37
18	0.235	0.063	32.33	1.99	318.88
19	0.364	0.097	31.25	1.87	531.65
20	0.409	0.109	31.83	1.98	646.00
21	0.458	0.122	32.55	2.03	733.91
22	0.588	0.156	31.86	2.05	738.46
23	0.748	0.199	31.92	2.03	683.04
24	3.563	0.948	31.72	2.08	672.94
25	2.722	0.724	32.08	1.13	664.47
26	2.064	0.549	31.87	2.45	649.87
27	1.548	0.412	32.43	2.59	619.03
28	2.134	0.568	33.90	2.16	676.49
29	2.492	0.397	33.12	2.23	584.91
30	1.963	0.256	33.19	1.43	602.14
31	0.963	0.256	33.43	2.51	602.14
32	0.984	0.262	33.32	2.55	608.86
33	1.066	0.284	32.15	2.18	674.94
34	2.409	0.375	31.30	2.21	717.60
35	1.138	1.101	31.92	2.10	746.64
36	1.325	0.353	32.98	2.51	659.76
37	1.106	0.294	32.62	2.59	626.70
38	1.034	0.275	32.43	2.61	651.65
39	0.841	0.224	31.94	2.34	728.05
40	0.937	0.249	32.22	2.54	690.55
41	0.951	0.253	30.48	2.13	700.62
42	1.597	0.425	29.30	1.95	703.88
43	2.233	0.594	29.78	1.94	645.32
44	3.242	0.863	30.32	1.49	570.53
45	2.615	0.696	31.44	1.15	613.54

46	2.021	0.538	31.93	1.92	638.33
47	0.635	0.169	32.41	2.24	598.43

Table 4.1 continued.			Tabulated experimental data		
48	3.960	1.054	33.00	1.59	536.94
49	4.318	1.149	31.89	1.22	516.38
50	2.317	0.616	31.10	1.83	546.81
51	1.187	0.316	32.11	2.17	634.28
52	1.105	0.294	31.27	2.13	636.04
53	1.788	0.476	30.40	1.96	587.60
54	3.328	1.684	29.72	1.93	600.43
55	3.581	0.953	28.00	1.09	638.52
56	2.262	0.602	27.52	1.89	681.74
57	1.512	0.402	28.20	2.49	717.48
58	0.924	2.108	27.87	1.86	722.50
59	2.362	2.225	27.92	2.76	225.06
60	0.685	0.980	27.43	1.75	672.85
61	0.818	0.218	26.65	2.65	646.12
62	0.442	1.820	27.97	2.56	684.47
63	1.152	1.903	28.15	1.94	597.99
64	1.670	1.509	28.69	1.86	614.43
65	3.291	0.876	27.23	1.84	604.79
66	5.124	1.097	26.93	1.51	658.78
67	2.251	0.599	26.44	1.98	717.02
68	1.831	0.487	27.53	2.90	721.13
69	2.481	0.660	28.45	1.73	643.82
70	5.321	2.746	27.73	1.24	515.85
71	5.006	3.993	26.16	1.30	565.38
72	4.228	2.987	26.95	1.32	562.16
73	3.842	2.459	26.23	1.50	621.78
74	4.076	1.085	25.13	1.40	609.16
75	2.635	0.701	27.67	1.81	636.64
76	1.780	0.474	29.08	1.91	649.79
77	2.727	0.726	30.21	1.87	627.37
78	2.675	0.712	30.53	1.49	618.79
79	2.430	0.647	30.16	1.91	680.59
80	2.036	0.542	31.15	1.98	710.05
81	1.686	0.449	32.48	2.42	725.34

82	2.244	0.597	32.66	2.21	587.34
83	1.905	0.507	34.58	2.70	652.07
84	1.112	0.296	32.83	2.81	707.77
85	0.282	0.075	33.03	2.90	719.17
86	0.792	0.211	33.47	2.50	714.66
Table 4.1 continued.			Tabulated experimental data		
87	0.890	0.237	32.45	2.25	712.73
88	0.707	0.188	31.59	2.00	737.00
89	0.692	0.184	31.15	1.88	733.81
90	1.013	0.270	31.36	2.10	750.55
91	1.095	0.291	32.67	2.15	741.19
92	1.041	0.277	32.60	2.40	707.73
93	1.079	0.287	34.40	2.16	689.61
94	0.798	0.212	34.99	2.19	739.71
95	0.890	0.237	35.57	2.52	731.61
96	0.909	0.242	35.45	2.39	686.61
97	0.820	0.218	35.97	2.32	674.29
98	0.613	0.163	35.58	2.29	704.38
99	0.689	0.183	35.68	2.32	705.89
100	0.657	0.175	35.67	2.42	679.48
101	0.844	0.145	35.99	2.51	559.57
102	0.698	0.186	36.30	2.12	694.22
103	0.622	0.165	35.58	2.20	670.80
104	0.925	0.246	34.98	2.18	632.88
105	0.824	0.326	36.30	2.52	670.80
106	0.801	0.232	36.43	2.50	756.63
107	0.815	0.230	36.24	2.54	711.73
108	1.574	0.419	35.10	2.42	732.38
109	1.969	0.311	35.33	1.44	787.22
110	2.613	1.493	36.10	1.45	775.99
111	2.658	1.772	34.60	1.42	720.45
112	2.974	2.388	28.89	2.04	326.41
113	0.507	0.135	32.07	1.89	738.03
114	0.842	0.224	32.30	1.80	760.08
115	1.054	0.280	31.61	1.75	759.71
116	0.966	0.257	32.10	2.12	835.62
117	0.882	0.235	32.67	2.15	870.85
118	0.847	0.225	32.36	2.25	842.84

119	3.040	0.809	30.75	1.53	777.87
120	1.422	0.378	31.75	2.12	777.31

4.2 OBJECTIVE 2

To determine the effect of atmospheric dust on the energy capture efficiency of the solar panel.

4.2.1 RESULTS AND DISCUSSION

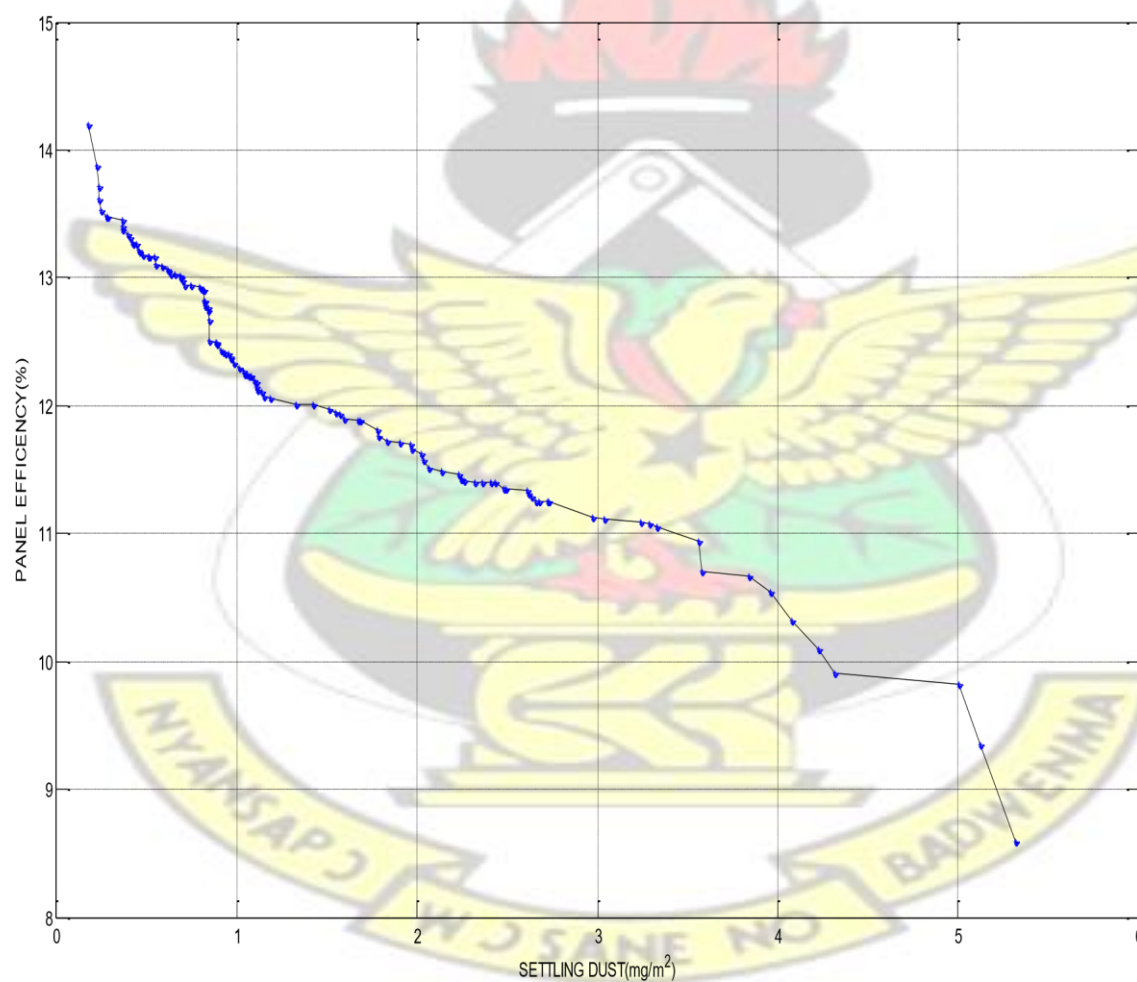


Figure 4.1. The effect of dust on panel efficiency

From the experimental data, the accumulated daily loss of panel efficiency was 15.9 %, averaging 0.13 % in a day. The accumulation of dust particles on the surface of photovoltaic (PV) panel greatly affects its performance especially in these dusty areas. The settling dust decreases the scatters sunshine radiation in the atmosphere before reaching the panel and consequently decreases the useful energy received by the panels leading to degradation in the panel's efficiency as shown in figure 4.1.

4.3 OBJECTIVE 3

To determine the effect of settled dust on the current and voltage outputs of the panel.

4.3.1 RESULTS AND DISCUSSION

Effect of Settling Dust on the Current Outputs of the Panel

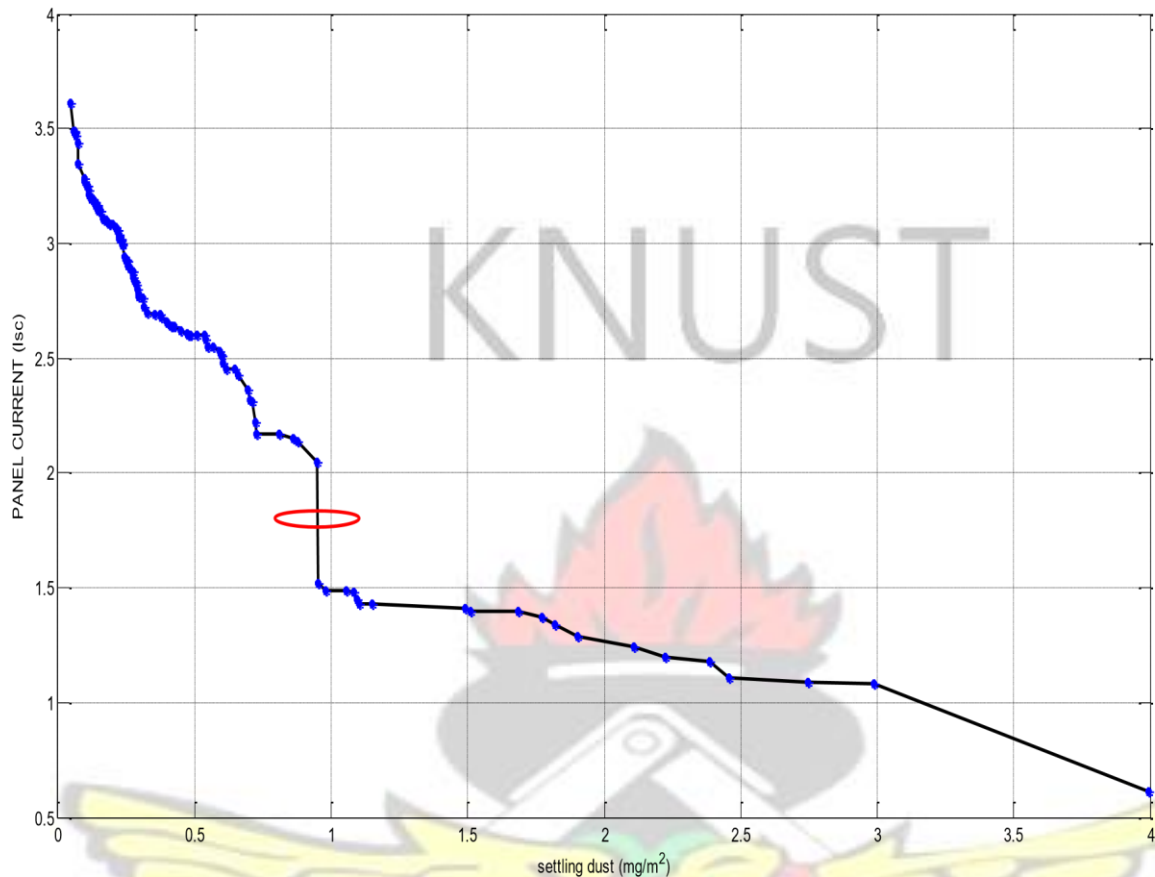


Figure 4.2 Impart of settling dust on current output

Solar panel gets degraded day to day by dust deposition over long exposure, as short circuit current (I_{sc}) is proportional to solar irradiance which was mainly affected by settling dust. The graphical results in figure. 4.2, shows that an increase in dust settlement on the panel resulted in a relative decrease in current output. From the short-circuit current (I_{sc}) profile, a steady step height was observed at about 95 days (marked on figure). This height indicated the period where the dust load on the panel was assumed to reach constant. After this period, most of the dust settling on the panel was resuspended to the atmosphere by the wind current. The current output of the panel after this period didn't change significantly but its miniscule variations was based on relative changes in dust concentrations in the atmosphere. A least value of 0.6A was measured as current output. There was a total reduction of the short circuit current by 16.6%

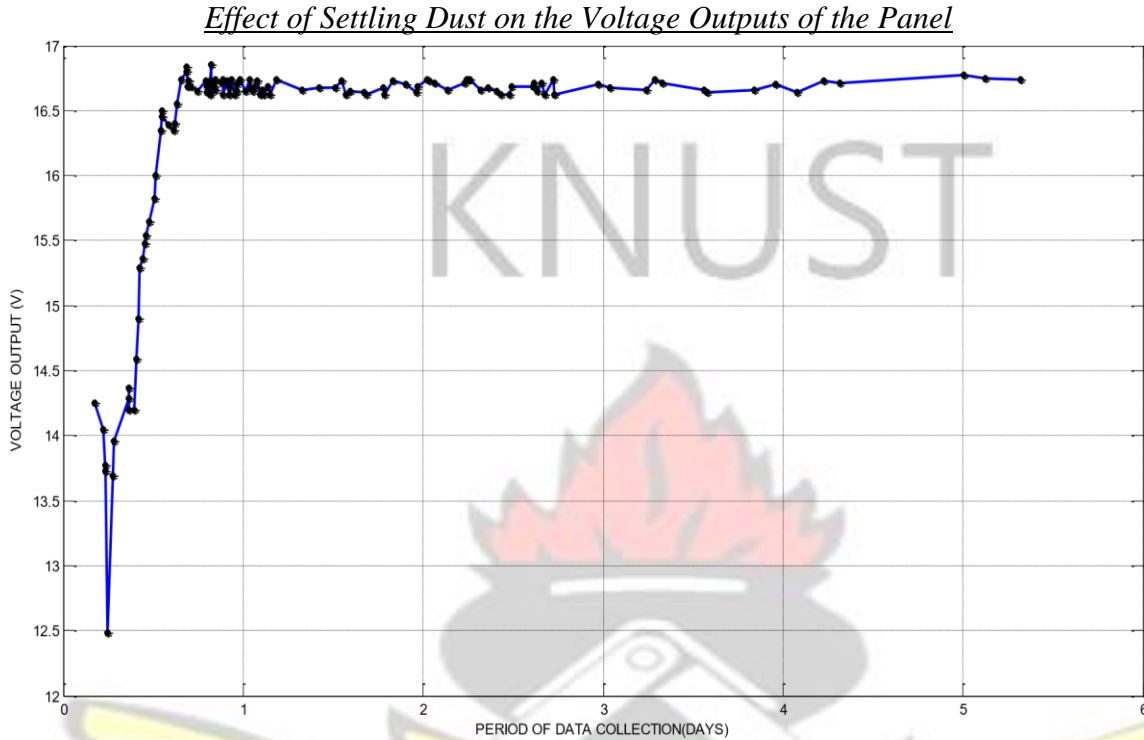


Figure 4.3 Factors that influences panel voltage output

At a given intensity, a solar panel's operating voltage is determined by the characteristics of the load and the temperature of the panel. These factors are not influenced by dust. As the panel uses a battery system for storage, the battery's internal resistance will dictate the module's operating voltage. Dust settlement on the panel surface did not affect the voltage output. From figure 4.3, the voltage initially dropped significantly because of the battery internal resistance and then resumed its nominal operating voltage i.e. 16-17 V. It remained almost constant but responded linearly with slight variations in panel temperature.

The Current Voltage ($I - V$) Curve Representation from Measured Data

The $I - V$ curve of a panel as shown in Fig. 4.4, describes its energy conversion capabilities at the existing conditions of irradiance (light level) and temperature.

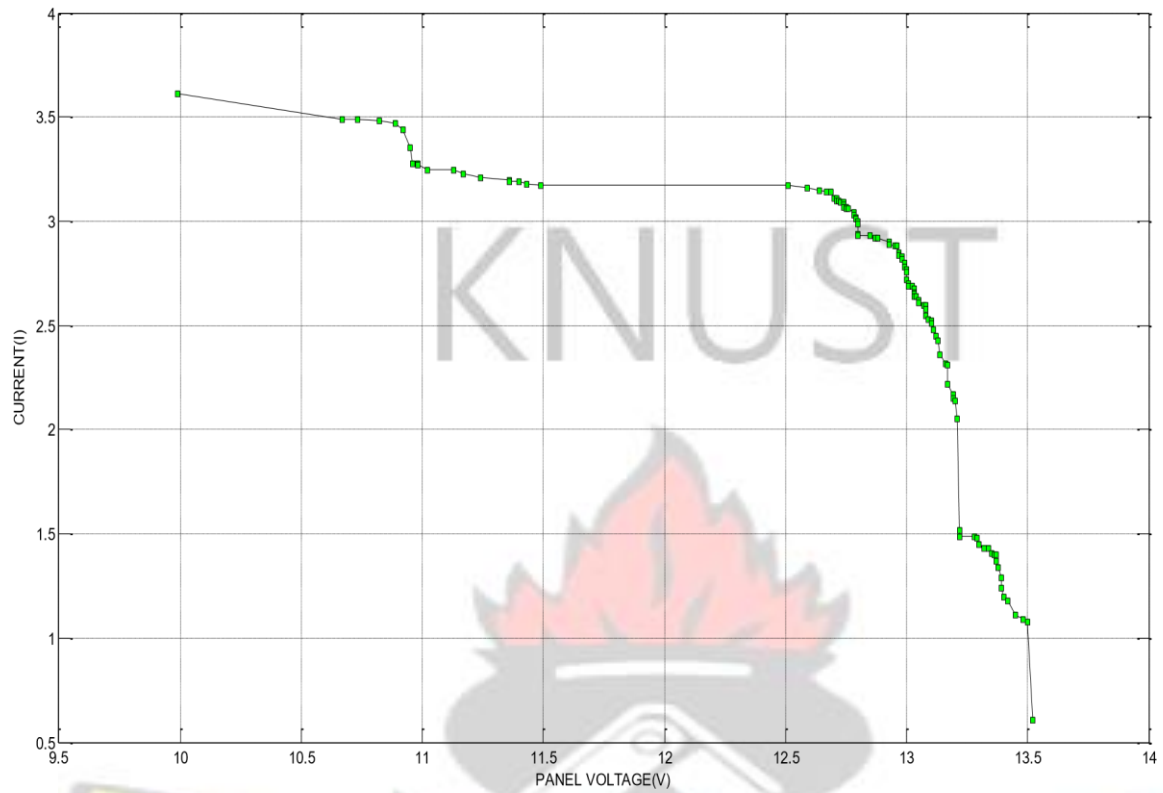


Figure.4.4. Experimental IV-Curve representation

4.4 OBJECTIVE 4

To graphically model the power output module of the panel

4.4.1 RESULTS AND DISCUSSION

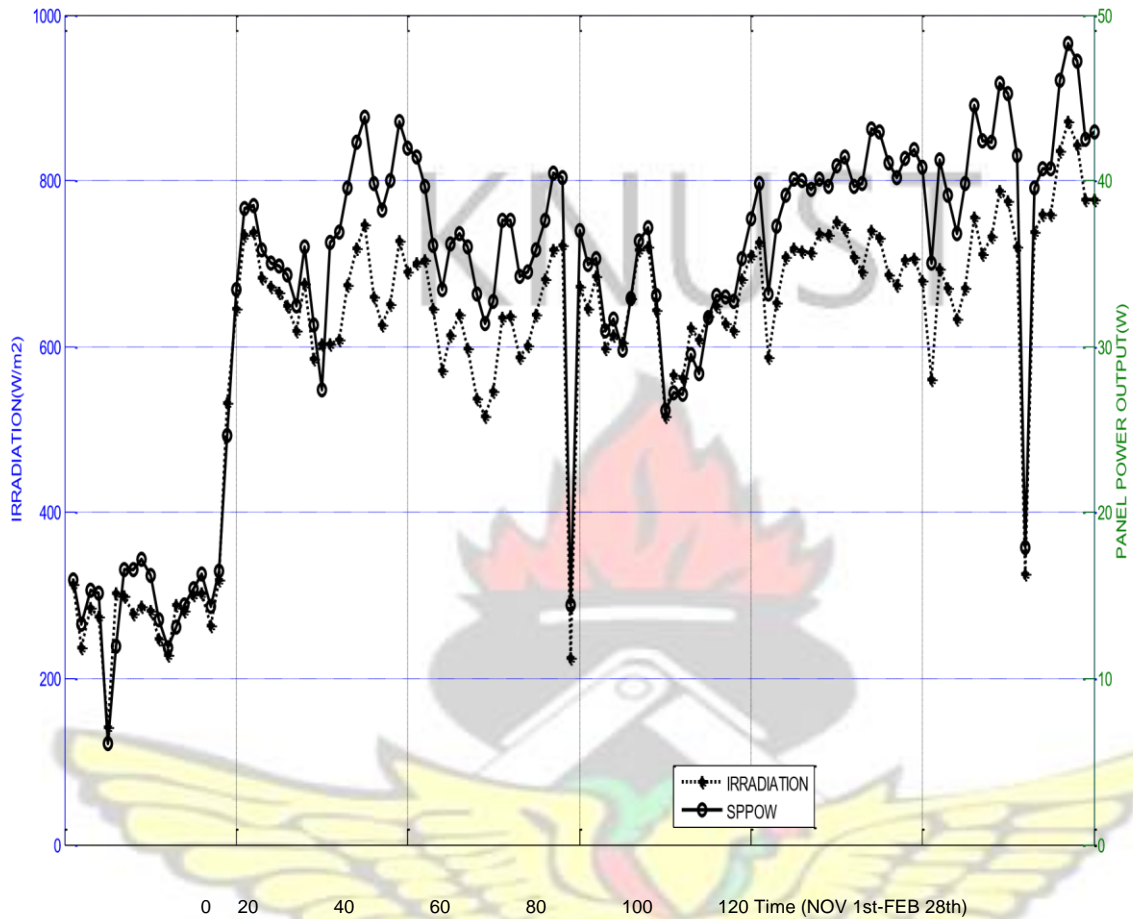


Figure.4.5. Relationship between Global Solar Irradiation and Panel Power Output

The daily variation in dust sampling at the project site lead to different transmittance of light radiation reaching the panel surface. Solar radiation output is a linear function of the current and power output of the panel i.e. power generated by a panel is dependent primarily on the availability of solar radiation. Thus, from figure 4.5, panel power output responded linearly to increasing and decreasing values of solar irradiation values.

4.5 OBJECTIVE 5

To model the effect of sampled atmospheric dust particles and wind speed on the panel power output

4.5.1 RESULTS AND DISCUSSION

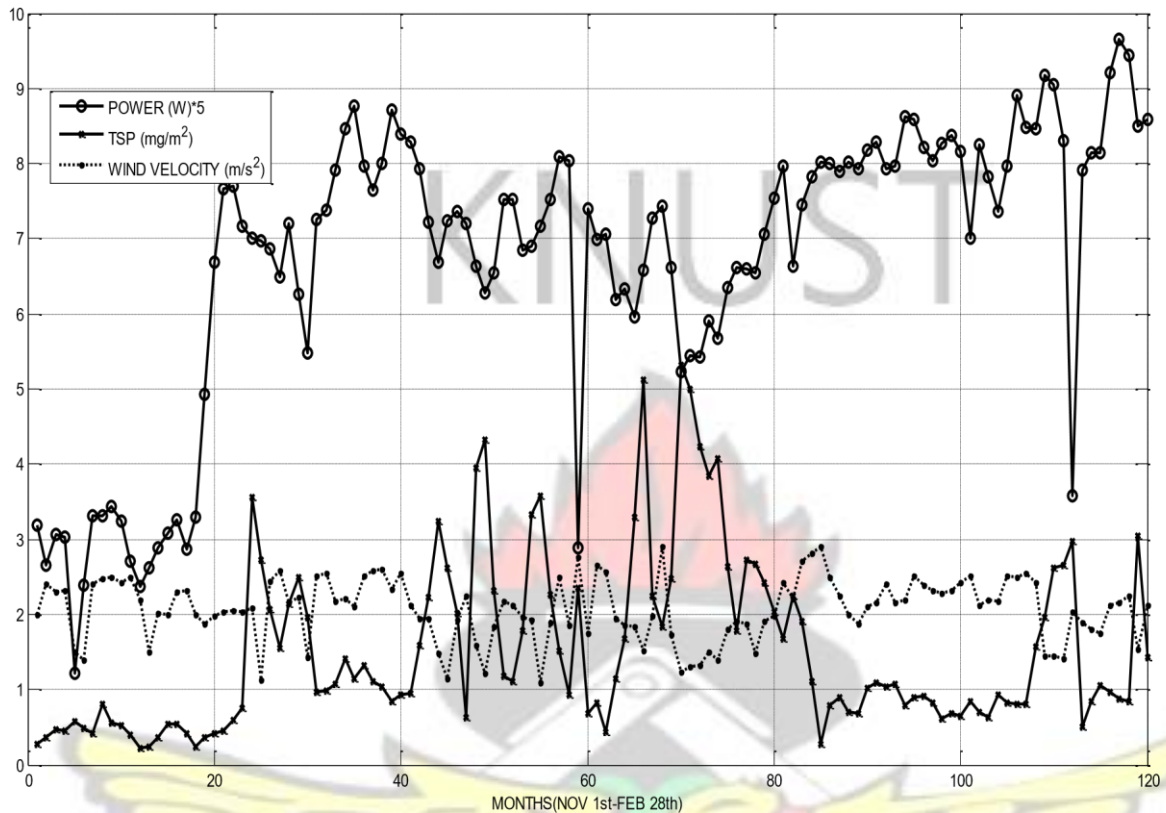


Figure 4.6 Effect of settling dust and wind velocity on panel power output.

Atmospheric dust eventually settles on panel surfaces, creating a fine layer of accumulated dust. Different parameters are reported to influence dust accumulation such as gravitational forces, wind speed, wind direction and the wetness of the surface. Of those parameters, the most dominating ones are the gravitational effect (settling velocity of dust) and wind speed. In figure 4.6, relatively low wind speeds increases the deposition of dust thus reducing power output of the panel while high wind speeds helps to remove dust from panel surface by convective means which depends also on the tilt angle of the panel and the wind direction. For the first 20 days, sun radiation was relatively low because of cloudy conditions.

4.5.2 MODELLING THE EFFECT OF SAMPLED ATMOSPHERIC DUST PARTICLES AND WIND SPEED ON THE PANEL POWER OUTPUT

By the methods of least squares with 3 variables;

$$\begin{aligned}\sum P &= Na_0 + a_1 \sum D + a_2 \sum V \\ \sum PD &= a_0 \sum D + a_1 \sum D^2 + a_2 \sum DV \\ \sum VP &= a_0 \sum V + a_1 \sum DV + a_2 \sum V^2\end{aligned}$$

N=120; (number of days)

$$4036.74 = 120a_0 + 200.16a_1 + 255.1a_2 \quad (4.4)$$

$$6736.99 = 200.16a_0 + 844.11a_1 + 389.28a_2 \quad (4.5)$$

$$8654.31 = 255.1a_0 + 389.28a_1 + 554.44a_2 \quad (4.6)$$

Simplifying the 3 equations above and solving for a_0, a_1, a_2 values;

$$a_0 = 16.309, a_1 = 0.5546, a_2 = 7.717$$

Therefore, the equation comes out to be as compared with equation (4.3);

$$P = 16.309 + 0.5546D + 7.717V \quad (4.7)$$

Where P, D, V are three variables, D and V are considered to be independent variables and P, the dependent variable. To test the validity of the equation derived above, Table 4.2 gives value of η measured and calculated.

Table.4.2. Values of η measured and calculated

Months	P measured (from measured values)	P calculated (calculated from equation)	Difference of the two η values
NOVEMBER	22.06	16.89299	5.16701
DECEMBER	36.90	43.73126	-6.831258

JANUARY	34.80	31.94066	2.859337
FEBUARY	41.11	41.97005	-0.860045
	$\sum \eta 1 = 134.87$	$\sum \eta 2 = 134.535$	

Multiple Correlation Coefficient:

$$R = \frac{\sum n1 * \sum n2}{\sqrt{[\sum n1^2 * \sum n2^2]}} \quad (4.11)$$

$$R = \frac{134.87 * 134.535}{\sqrt{[134.87^2 * 134.535^2]}} \quad (4.12)$$

$$R = \frac{18144.74}{18177.74} = 1 \quad (4.13)$$

According to the properties of multiple correlation coefficient, if the value of R (multiple correlation coefficients) comes out to be unity (1), then the observed and expected value obtained for the power output of module (P) coincide and the observed (P) is a linear function of V and D.

An R - code (software modeling) was written and referred in Appendix C Linear Regression Method with a Mathematical Modeling Software, R, expressed the intercept of the linear expression as 28.089 and the coefficients of D and V as -575.263 and 8.408 respectively. The linear equation can be expressed;

$$P = 28.089 - 575.263 D + 8.408 V \quad (4.14)$$

Where P (Power - W) is a dependent variable and a linear function of the independent variables D (Settling dust – mg/m³), V (velocity - m/s²).

The two modeled power output equations by the linear regression analysis was compared to the measured power output of the panel on the same graph as shown in figure 4.7. It is observed that the profile of power output by the software model has its data points close to the measured values of power.

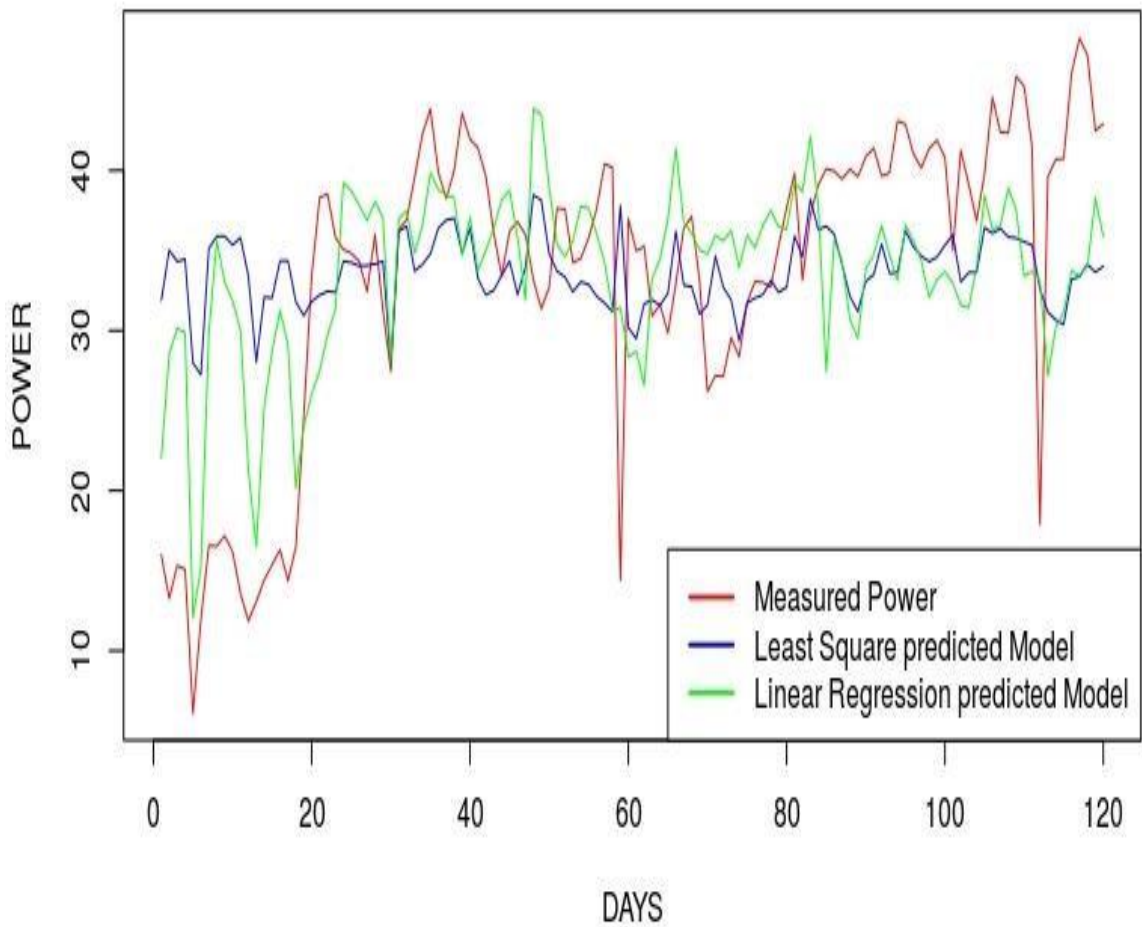
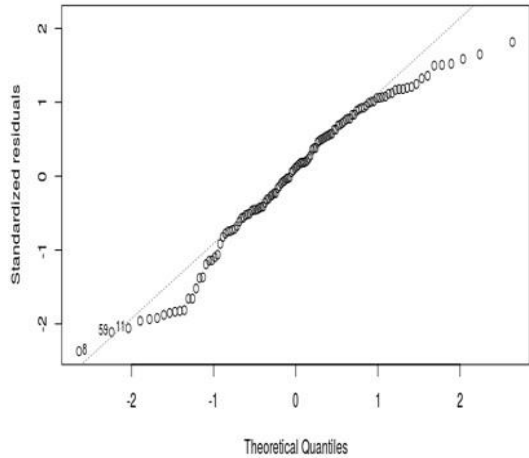
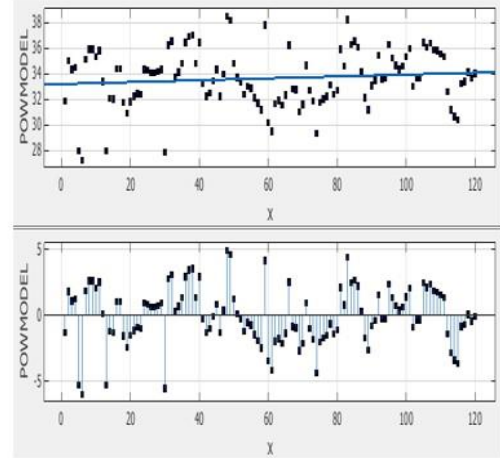


Figure 4.7 Comparing the power output of the panel (mathematical modules and measured data)



a) Software Regression analysis



b) Least square of 3 variables

Figure 4.8 Residual plots of the linear modules

The quanta – quanta (Q-Q) plot of residual of the linear regression in figure 4.8, shows the regression model of the software model is almost normal (line of best fit passes through most of the data points) compared to the residual plots the least square methods where the data points deviates a lot from its line of best fit.

The mathematical model with the software, R, was considered as the best model with its independent variables as wind velocity, V , and Settling dust, D , and how these variables affects the power output of the panel.

CHAPTER FIVE

5.0 CONCLUSION AND RECOMMENDATION

In this thesis, the effect of settling dust on PV panel under the influence of these external factors, i.e. radiation, temperature and wind was studied. This work investigated mainly the effect of settling dust (atmospheric dust) on sun radiation reaching the panel surface, thus the effect on panel power output.

The effect of dust is accumulative, i.e. panel performance is reduced by increasing dust settlement over time or until it was manually cleaned by rain. Rainfall was recorded only on the 20th of Feb, 2015 between 1-4pm during the period of studies. The dust load was observed to remain constant on the panel at 95 days in figure 4.2 but wasn't quantified (weighed). During the period of study, the amount of dust that settled on the panel surface was controlled by the varying tilt angles of the panel i.e. relatively less amount of dust was observed on the panel. The tilt angle of the PV installation plays a major role in the amount of dust accumulated on the devices, where higher tilt angles decreases dust concentrations on the panel and vice versa.

To conclude, dust must be removed from the surface of solar PV panel by appropriate cleaning methods in order to ensure maximum performance, given the fact that it has a short lifespan.

5.1 CONCLUSIONS

From the experimental results, the following conclusions can be obtained:

1. Increasing amount of dust in the atmosphere resulted in a relative decrease in current and power output.
2. The open circuit voltage of the panel is independent on settling dust.
3. Settling harmattan dust affected significantly the performance of panel by reducing its power output by 28.7% and panel efficiency by 5.6%.

5.2 RECOMMENDATIONS

- To maximize the output of solar PV module and reduce the degradation caused by airborne dust accumulation, frequently cleaning is strongly recommended especially for these drought areas (Walewale) to maintain the maximum efficiency of the panel
- The physical characteristics of the harmattan dust must be determined and correlated to the observed effects.
- Dust Accumulation and Distribution Uniformity on Photovoltaic Modules: The non-uniform settlement of dust on PV modules provides further complication in the matter of determination of losses due to dust. These effects of non-uniformity was mainly caused by varying tilt angle with the solar tracker mechanism and wind direction with respect to the angle of tilt.

REFERENCES

1. Al-Hasan, A. Y (1998), *A new correlation for direct beam solar radiation received by photovoltaic panel with sand dust accumulated on its surface*" Solar Energy, 63 (5), pp. 323–333.

2. Allen, T (1981), *Particle size measurement*, 3rd ed. Chapman & Hall.
3. Bowling, R. A (1988). *A theoretical review of particle adhesion*, In: Mittal KL, editor. *Particles on surfaces*, Vol. 1. New York: Plenum Press. pp 129–142.
4. Contreras, M. A (2006), *Characterization of Cu (In, Ga) Se₂ materials used in record performance solar cell*, *Thin Solid Films*; 511:51–4.
5. Dietz, A. G (1963), *Introduction to the utilization of solar energy*. In *Diathermassous Material and Properties of Materials*, Zarem, A.M and Erway D.D (Eds), McGraw Hill, New York.
6. Elminir, H. K., Ghitass A. E (2006), "*Effect of dust on the transparent cover of solar collectors.*" *Energy Conversion and Management* 47(18-19): 3192-3203.)
7. Gevorkian P (2012), *Large scale solar power systems: Construction and economics*, Cambridge University Press
8. Goetzberger, A., Hebling, C and Schock, H. W (2003), *Photovoltaic materials: history, status and outlook*, *Materials Science and Engineering R: Reports*; 40 (1): 1–46.
9. Goossens, E. D and Kerschaever Van (1999), *Aeolian dust deposition on photovoltaic solar cells: the effects of wind velocity and airborne dust concentration on cell performance*, *Solar Energy*, 66 (4), pp. 277–289.
10. Hinds, C. W (1999), *Aerosol technology: Properties, behavior, and measurement of airborne particles*, John Wiley & Sons Inc. New York. pp 42-74.
11. Hottel, H and Woertz, B (1942), *Performance of flat-plate solar-heat collectors*, *Transactions of the American Society of Mechanical Engineers (USA)*, p. 64.
12. IEA Renewable Energy Working Party (2002), *Renewable Energy. into the mainstream*, p 9.

13. International Energy Agency (2012), *Energy Technology Perspectives 2012*.
14. Jager-Waldau, A (2011), *Progress in chalcopyrite compound semiconductor research for photovoltaic applications and transfer of results into actual solar cell production*, Solar Energy Materials and Solar Cells; 95(6):1509–17.
15. Kalogirou, S. A and Tripanagnostopoulos, Y (2007), *Industrial application of PV/T solar energy systems*. Applied Thermal Engineering; 27(8–9):1259–70.
16. Krupp, H, Adv. Colloid Interface Sci., 1(2), 111 (1967). IN: Bowling, R. A, *Theoretical Review of Particle Adhesion*, Texas Instruments Incorporated, Materials Science Laboratory.
17. Mahowald, N. M, Baker (2005), *Atmospheric global dust cycle and iron inputs to the ocean*, Global Biogeochemical Cycles, VOL. 19, GB4025.
18. Malay, K. Mazumder (2013), *Self Cleaning solar panel and concentrators with transparent electrodynamic screens*, EP 2647057A2. Google patent
19. Mani, M and Pillai, R (2010), *Impact of dust on solar photovoltaic (PV) performance: research status, challenges and recommendations*, Renewable and Sustainable Energy Reviews, 14 (9), pp. 3124–3131.
20. Marcelo, Gradella Villalva, et al. (2009), *Comprehensive Approach to Modeling and Simulation of Photovoltaic Arrays*, IEEE Transaction on Power Electronics, Vol. 24, No. 5, Pg.1198-1204).
21. Markvart, T and Castaner, L (2003), *Practical Handbook of Photovoltaics, Fundamentals and Applications*, Elsevier, 2003.
22. Massey, B. S (1994). *Mechanics of fluids*, Chapman & Hall UK. pp 172
23. Meral, M. E and Dinc, F (2011), *A review of the factors affecting operation and efficiency of photovoltaic based electricity generation systems*, Renewable and

Sustainable Energy Reviews 2011; 15(5): 2176–84

24. Pye, K (1989), *Aeolian Dust and Dust Deposits*, Academic Press, New York.
25. Rajiv, Kohli and Kashmiri, Mittal (2012) *Developments in Surface Contamination and Cleaning: Methods for Removal of Particle Contaminants*, William Andrew, Elsevier, Volume Three.
26. Razykov, T. M, *Solar photovoltaic electricity: current status and future prospects. Solar Energy*, 2011; 85(8):1580–608.
27. Shaharin, A., Haizat, H., Nik - Suti, Mohd, S. I (2011), *Effect of dust on the performance of PV panels*. World academy of Science, Engineering and Tech., 58
28. Shao, Y (2008), *Physics and Modelling of Wind Erosion*, Springer, 2008.
29. Skoplaki, E and Palyvos, J. A (2009), *On the temperature dependence of photovoltaic module electrical performance: a review of efficiency/power correlations*, *Solar Energy* 2009; 83(5):614–24.
30. Sunnu, A. K (2006), *An experimental study of the Saharan dust physical characteristics and fluxes near the Gulf of Guinea*, PhD Thesis, Universite du Sud Toulon-Var, France
31. <http://www.rise.org.au/info/Education/SAPS/sps003.html>. (15/02/2010)
32. <http://www.pveducation.org/pvcdrom/modules/nominal-operating-celltemperature>. (Accessed 16/01/2015)
33. Available from: <http://www.blueplanet-energy.com/images/solar/PV-cellmodule-array.gif>. [18 September 2014].
34. Solar panel edited by Rfassbind, Available from: http://en.wikipedia.org/wiki/Solar_panel. [25 November 2014].

35. Photovoltaic system edited by Julesd, Available from: <http://en.wikipedia.org/wiki/Photovoltaic_system>. [20 July 2014].

KNUST

APPENDIX A

% Compute cell's current (A) from voltage (V), suns (suns) & temp (°C)

% "Model of Photovoltaic Module in Matlab™", function

Ia = solar(Va,Suns,TaC)

% Ia,Va = current and voltage vectors (A) and (V)

% G = number of Suns (1 Sun = 1000 W/m²)

% T = temperature of the cell (°C) k = 1.38e-

23; % Boltzmann constant (J/K) q = 1.60e-19;

% Elementary charge (C) n = 1.2; % Quality factor for the diode

Vg = 1.12; % Voltage of the Crystalline Silicon (eV)

T1 = 273 + 25; % Normalised temperature (K)

$V_{oc_T1} = 21.02$; % Open-current voltage at T1 (V).
 $I_{sc_T1} = 3.62$; % Short-circuit current at T1 (A) K_0
 $= 0.06$; % Current/Temperature coefficient (A/K).
 $dVdI_Voc = -0.155$; % dV/dI coefficient at V_{oc} (A/V).
 $TaK = 273 + TaC$; % Convert cell's temp from °C to K
 $IL_T1 = I_{sc_T1} * S_{uns}$; % Compute IL at T1. Equation (2.2)
 $IL = IL_T1 + K_0 * (TaK - T1)$; % Apply the temp effect. Equation (2.5)
 $I_{0_T1} = I_{sc_T1} / (\exp(q * V_{oc_T1} / (n * k * T1)) - 1)$; % Equation (2.9)
 $I_0 = I_{0_T1} * (TaK / T1)^{(3/n)} * \exp(-q * V_g / (n * k) * ((1 / TaK) - (1 / T1)))$; % (2.4)
 $X_v = I_{0_T1} * q / (n * k * T1) * \exp(q * V_{oc_T1} / (n * k * T1))$; % Equation (2.11)
 $R_s = -dVdI_Voc - 1 / X_v$; % Compute the R_s Resistance. Equation (2.10)
 $V_{t_Ta} = n * k * TaK / q$; $I_a = \text{zeros}(\text{size}(V_a))$; % Initialize I_a vector
 % Compute I_a with Newton method for $j=1:5$; $I_a = I_a - (IL - I_a - I_0 * (\exp((V_a + I_a * R_s) / V_{t_Ta}) - 1)) / (-1 - (I_0 * (\exp((V_a + I_a * R_s) / V_{t_Ta}) - 1)) * R_s / V_{t_Ta})$; end end

APPENDIX B

COMPARING EXPERIMENTAL RESULTS OF WIND SPEED AND SOLAR IRRADIATION WITH RETSCREEN DATA FOR THE NORTHERN REGION OF GHANA

SOURCE (RETSCREEN Software, NASA 2010)

AVG MONTHLY DATA	November	December	January	February
WIND SPEED (m/s)	2.10	2.10	2.60	2.10
RADIATION (KWh/m ² /d)	5.44	4.76	5.13	5.55

SOURCE (Average monthly experimental values, November to February)

DATA	November	December	January	February

WIND SPEED (m/s)	2.10	2.18	2.55	2.25
RADIATION (KWh/m ² /d)	3.40	5.04	5.30	5.72
DUST (mg/m ³)	0.81	1.78	3.03	0.96

APPENDIX C

R code to model the effect of dust and wind on power output of a panel

```

*bob1=read.table("/home/jesse/Desktop/data1.csv",header=T)      # Reads data into R
*m1=lm(bob1$SP_POW. ~ bob1$WIND + bob1$DUST) # generates linear regression
model for power generated and wind and dust as explanatory variables. summary(m1)
*plot(bob1$DAYS,bob1$SP_POW.,col="red",type = "l",xlab = "DAYS",ylab =
"POWER")                #      Plots      power      against      days
*lines(bob1$DAYS,bob1$P_POW,col="blue",type = "l")              # plots least square
predicted power against day on the same graph
*lines(bob1$DAYS,bob1$PP_POWER,col="green",type="l") # plots linear regression
predicted power against day on the same graph
*legend("bottomright",c("Measured Power","Least Square predicted Model","Linear
Regression predicted Model"),col=c("red","blue","green"), lwd=2)

```

RESULTS

Call:

lm(formula = bob1\$SP_POW. ~ bob1\$WIND + bob1\$DUST)

Residuals:

Min	Median	Max
-19.1813	0.9464	14.7682

Coefficients:

	Estimate	Std. Error	t value	Pr(> t)
(Intercept)	28.089	5.159	5.445	2.90e-07 ***
bob1\$WIND	8.408	2.374	3.542	0.000571 ***
bob1\$DUST	-575.263	87.322	-6.588	1.34e-09 *** ---

Residual standard error: 8.17 on 117 degrees of freedom

Multiple R-squared: 0.2992, Adjusted R-squared: 0.2872 #95% confidence bounds

